

# **SECURITY**

---

# **MARKING**

**The classified or limited status of this report applies to each page, unless otherwise marked.**

**Separate page printouts MUST be marked accordingly.**

---

**THIS DOCUMENT CONTAINS INFORMATION AFFECTING THE NATIONAL DEFENSE OF THE UNITED STATES WITHIN THE MEANING OF THE ESPIONAGE LAWS, TITLE 18, U.S.C., SECTIONS 793 AND 794. THE TRANSMISSION OR THE REVELATION OF ITS CONTENTS IN ANY MANNER TO AN UNAUTHORIZED PERSON IS PROHIBITED BY LAW.**

**NOTICE: When government or other drawings, specifications or other data are used for any purpose other than in connection with a definitely related government procurement operation, the U. S. Government thereby incurs no responsibility, nor any obligation whatsoever; and the fact that the Government may have formulated, furnished, or in any way supplied the said drawings, specifications, or other data is not to be regarded by implication or otherwise as in any manner licensing the holder or any other person or corporation, or conveying any rights or permission to manufacture, use or sell any patented invention that may in any way be related thereto.**

## **DISCLAIMER NOTICE**

**THIS DOCUMENT IS BEST QUALITY  
PRACTICABLE. THE COPY FURNISHED  
TO DTIC CONTAINED A SIGNIFICANT  
NUMBER OF PAGES WHICH DO NOT  
REPRODUCE LEGIBLY.**

AFRPL-TR-65-213

AD 474229

## SOLID PROPELLANT IGNITION STUDIES

*Final Report*  
*November 5, 1965*

AIR FORCE ROCKET PROPULSION LABORATORY  
RESEARCH AND TECHNOLOGY DIVISION  
AIR FORCE SYSTEMS COMMAND  
EDWARDS, CALIFORNIA

CONTRACT NO. AF 04(611)-10534  
PROGRAM STRUCTURE NO. 750G  
PROJECT NO. 3059

*SRI Project No. FRU-5354*

*By*

NORMAN FISHMAN

STANFORD RESEARCH INSTITUTE  
MENLO PARK, CALIFORNIA

Copy No. ....71....

## FOREWORD

This report was prepared under Project No. 3059, Program Structure No. 750G, Contract No. AF 04(611)-10534, by Stanford Research Institute, Menlo Park, California. Lt. Charles E. Payne, RPMCP, AF Rocket Propulsion Laboratory, was the Air Force program monitor. Contractors project number was FRU-5354.

Inclusive dates of research were February 1 to September 1, 1965. The report was submitted by the author October 5, 1965.

The author wishes to thank Mr. C. M. McCullough and Mr. C. A. Kukkonen for their assistance in the conduct of the program.

This technical report has been reviewed and is approved.

Ralph W. Harned, Lt. Col., USAF  
Chief, Solid Rocket Division

## ABSTRACT

The ignition characteristics of five operational propellants and seven model systems of varying composition were investigated by the use of high flux radiant energy as the ignition stimulus. Our study has provided considerable information which relates ignition characteristics to compositional factors. Findings of particular importance are:

1. For the types of propellants studied, ignitability is directly related to burning rate; within each system, those factors which increase burning rate also ease ignition.
2. Minimum pressure for ignition of ammonium perchlorate propellants appears to be primarily related to the nature of the binder.

We examined the various theories of ignition and found that no model yet suggested has been adequately proved. In applying von Elbe's model, we showed that the observed pressure-dependency of ignition could be related to steady-state combustion characteristics of the propellant, and that thermal conduction into the subsurface material may contribute substantially to ignition time. We believe that we have placed the suggested mechanisms in proper perspective, so that identification can be made of the additional information required for fuller understanding of the important chemical processes.

## CONTENTS

ILLUSTRATIONS . . . . .	111
TABLES . . . . .	v
I INTRODUCTION . . . . .	1
II APPARATUS . . . . .	2
A. Radiant Energy Source . . . . .	2
B. Shutter Mechanism and Exposure Timing . . . . .	4
C. Flux Measurement . . . . .	8
D. Attenuation of Flux . . . . .	13
III EXPERIMENTAL PROGRAM . . . . .	15
A. Experimental Method . . . . .	15
B. Materials . . . . .	17
C. Test Results . . . . .	18
IV DATA ANALYSIS . . . . .	42
A. Discussion of Test Results . . . . .	42
B. Interrelationships among Compositional Characteristics and Ignition Characteristics . . . . .	45
C. Mechanisms of Ignition . . . . .	55
V SUMMARY AND CONCLUSIONS . . . . .	72
REFERENCES . . . . .	74

# ILLUSTRATIONS

<u>Figure</u>		<u>Page</u>
1.	Over-all View of Arc Image Furnace Facility. . . . .	3
2.	Interior View of Strong Electric Type 54007-1 Arc Lamp . . . . .	3
3.	Thermal Flux Profiles of the Arc Image . . . . .	5
4.	Photograph of Modified Shutter Mechanism . . . . .	6
5.	SRI Calorimeter for Flux Measurement . . . . .	9
6.	Hy-Cal Calorimeter before and after Blackening . . .	11
7.	Ignition Bomb with Hy-Cal Calorimeter in Stand-by Position. . . . .	12
8.	Two Positions for Placement of Flux-Attenuating Screens . . . . .	14
9.	Burning Rates of Model Propellant Compositions Prepared by SRI Propulsion Laboratory . . . . .	20
10.	Dependence of Exposure Time on Flux: PBAN-254 . . .	24
11.	Dependence of Exposure Time on Pressure: PBAN-254 . . . . .	25
12.	Dependence of Exposure Time on Pressure: PBAN-259 . . . . .	26
13.	Dependence of Exposure Time on Flux: PBAN-260 . .	27
14.	Dependence of Exposure Time on Pressure: PBAN-260 . . . . .	28
15.	Dependence of Exposure Time on Flux: PBAN-264 . . .	29
16.	Dependence of Exposure Time on Pressure: PBAN-264 . . . . .	30
17.	Dependence of Exposure Time on Pressure: PBAN-256 . . . . .	31
18.	Dependence of Exposure Time on Flux: PBAN-257 . . .	32

<u>Figure</u>		<u>Page</u>
19.	Dependence of Exposure Time on Pressure: PBAN-257 . . . . .	33
20.	Dependence of Exposure Time on Pressure: PBAN-258 . . . . .	34
21.	Dependence of Exposure Time on Flux: Pellet No. 3 (PBAN-254 solids) . . . . .	35
22.	Dependence of Exposure Time on Flux: ANB-3066 . . . . .	36
23.	Dependence of Exposure Time on Pressure: ANB-3066 . . . . .	37
24.	Dependence of Exposure Time on Pressure: ANB-3105 . . . . .	38
25.	Dependence of Exposure Time on Pressure: ANP-2677 . . . . .	39
26.	Dependence of Exposure Time on Pressure: ANP-2639AF . . . . .	40
27.	Dependence of Exposure Time on Pressure: ANP-2969KH-1 . . . . .	41
28.	Correlation between Burning Rate and Calculated Surface Temperature at Ignition. . . . .	53
29.	Dependence of Exposure Time on Flux: Calculated Times according to von Elbe's Model. . . . .	67
30.	Typical Relationship between Ignition Energy and Incident Flux . . . . .	69
31.	Relationship between Ignition Energy and Incident Flux: Data Calculated according to von Elbe's Model . . . . .	71



# TABLES

<u>Table</u>		<u>Page</u>
I	Model Propellant Compositions . . . . .	18
II	Results of Tests of Model Propellant Compositions . . .	21
III	Results of Tests of Pressed Pellets . . . . .	22
IV	Results of Tests of Propellant Compositions . . . . .	23
V	Thermal Responsivity of Compositions . . . . .	50
VI	Calculated Values of Surface Temperature . . . . .	51
VII	Weight Loss during Non-ignition Exposures . . . . .	61
VIII	Steady-State Flux and Preheat from von Elbe's Model . . . . .	65
IX	Input Data for Conduction Time Computations . . . . .	68

## I INTRODUCTION

Certain characteristics of propellants (such as percent oxidizer, particle size distribution, polymer pyrolyzability, and catalyst content) are known to have an influence on ignitability. By exploring the interrelationships among ignition characteristics and propellant compositional factors, one can determine how important each factor is to the ignition process. In addition, in the course of developing such information, the data taken over ranges of pressure and flux can be applied to studies of the mechanisms involved in the ignition process.

This program of ignition research was based on the use of high flux radiant energy as supplied by an arc image furnace, a technique first developed at Stanford Research Institute in 1957. Our work encompassed a systematic study of the variables governing ignition phenomena and examination of the possible controlling mechanisms. The objectives of the research under this contract were:

1. to determine interrelationships among ignition characteristics and propellant compositional factors
2. to evaluate the relative roles of solid decomposition, heterogeneous reaction, and gas phase mechanisms in the ignition process
3. to test the validity of various suggested theories of ignition.

## II APPARATUS

The arc image ignition furnace, constructed at Stanford Research Institute in 1957,<sup>1</sup> was considerably modified during the initial part of this program. A photograph of the over-all installation is shown in Fig. 1. A new arc lamp was installed to provide higher flux capability and greater operational stability of the arc. The rotating disc shutter was improved to provide better definition of the exposure pulse. The gas handling system was rebuilt to permit greater ease of operation as well as rapid depressurization for reducing the incidence of bomb rupture. Flux measuring procedures were refined and new methods for flux attenuation were instituted. These improvements provided us with a facility far superior to our previous apparatus; experimental results were obtained more readily over a wider range of conditions, and a higher degree of confidence in the accuracy of the data was achieved.

### A. Radiant Energy Source

The newly installed arc lamp is a Strong Excelite, Super 135, Type 54007-1, with 13.6-mm trim and 18-inch mirror. Care was taken to provide proper draft conditions for arc stability. Although the electrodes have considerable variability, continuous monitoring of arc current provides a record of intensity fluctuations which can be readily correlated with energy flux output. Normal operation is at a nominal arc current of 150 to 160 amperes. To obtain steady operation at the high current level, higher speed positive and negative electrode drive motors were required. An additional lamp modification, required to provide desired control capability, was a potentiometer to control the speed of the negative electrode drive motor. The interior of the lamp is shown in Fig. 2.

A thorough analysis of the focal volume and criticality of optical alignment was undertaken on another program.<sup>2</sup> The flux profiles were mapped with the use of a specially designed adjustable head so



FIG. 1 OVER-ALL VIEW OF ARC IMAGE FURNACE FACILITY

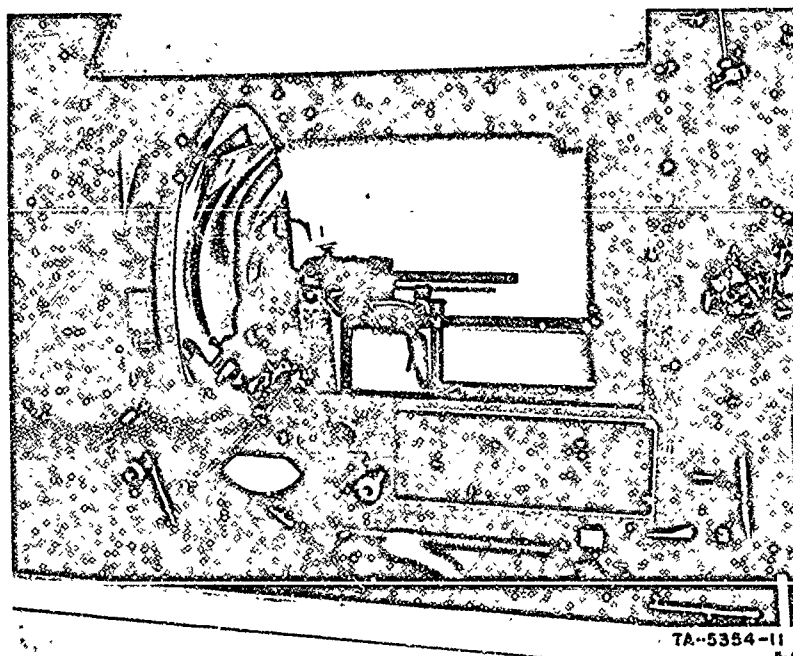


FIG. 2 INTERIOR VIEW OF STRONG ELECTRIC TYPE 54007-1  
ARC LAMP

that measurements could be made behind a half-glass without moving the glass with respect to the optical system; this provided a map of the thermal flux as seen by a specimen in the ignition bomb. The resulting flux profiles are shown in Fig. 3; the dimensions are shown in inches and the axes represent the lateral (X), vertical (Y), and axial (Z) directions. It can be seen that about 95 percent of the peak flux is available to a circular area about 0.1 inch in diameter.

#### B. Shutter Mechanism and Exposure Timing

A major disadvantage of the previous rotating-disc shutter mechanism<sup>1</sup> was the apparent movement of the image across the face of the specimen or calorimeter. The high-speed disc has previously been modified--the 2-inch circular opening had been elongated to a slot about 6 inches in length. Although this provided a trapezoidal pulse shape, with some 80 percent of the area of an equivalent square pulse, actual exposure times were only about 75 percent of calculated times due to the image displacement. The counter-rotating discs of the modified shutter do not shift the image, and radiant energy is applied to the same area during the entire time of exposure.

Each of the two counter-rotating discs has an elongated opening nominally 6 inches in length; both rotate at the same high speed. A third disc, with a 2-inch-diameter circular opening, is geared to the drive mechanism to rotate at 1/20th the speed of the high-speed discs. In this manner, one exposure on the optical axis is provided for each 20 revolutions of the high-speed discs. At maximum rotational speed this produces an interval of only about 0.7 second between exposures; therefore, a solenoid-operated leaf shutter was installed to provide for single exposures as needed. A cam-operated microswitch automatically actuates the leaf shutter for only one revolution of the slow disc; a relay must be reset after each exposure to obtain the next exposure. Figure 4 shows the open leaf shutter, the 2-inch aperture in the low-speed disc, and the aperture in the counter-rotating discs as it appears before it is fully open.

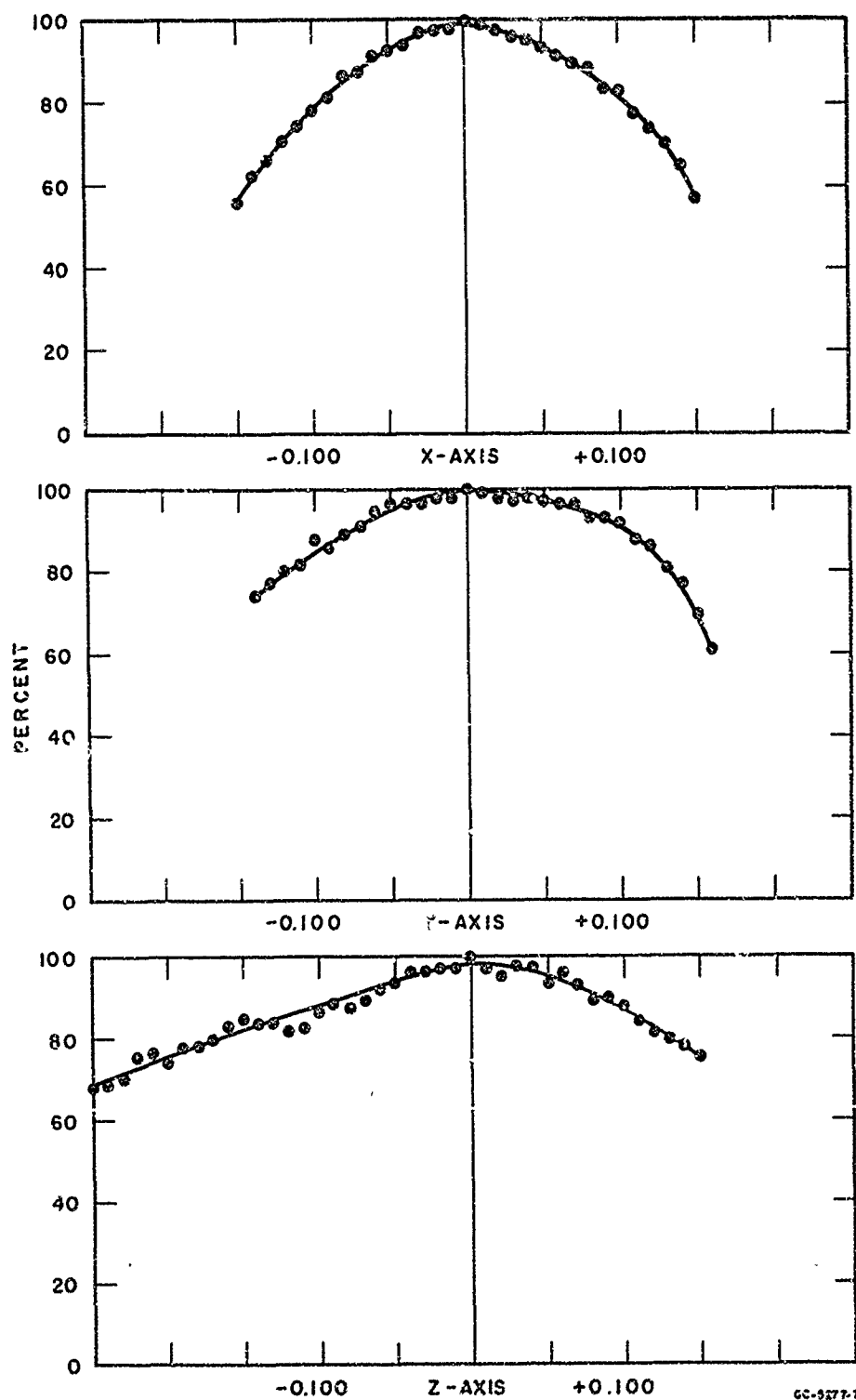


FIG. 3 THERMAL FLUX PROFILES OF THE ARC IMAGE

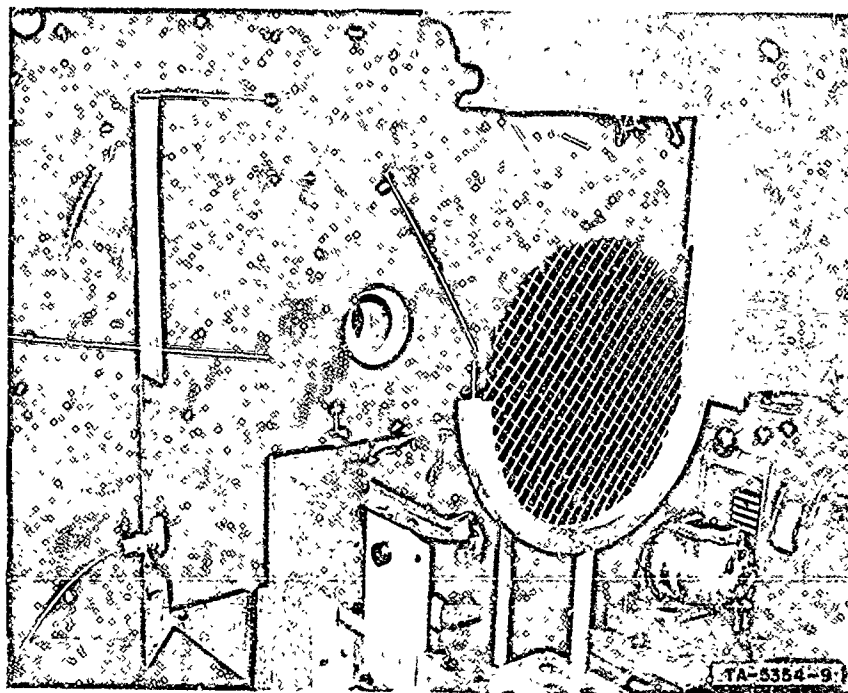


FIG. 4 PHOTOGRAPH OF MODIFIED SHUTTER MECHANISM

Rotational speed, and hence exposure time, is obtained (as before) from a calibrated indicating tachometer generator. As an auxiliary method for determining exposure time, an electronic counter, actuated by a magnetic switch at the high-speed discs, indicates the time for one revolution. These counts are made on a sampling basis; the last reading is a direct measure of the time for the one revolution during which exposure occurred. The system is integrated into the automatic solenoid shutter control so that the counter stops after exposure has occurred. The redundancy of time measurement thus provided does not unduly complicate equipment operation; the additional measurement can be used when desired, and confidence in exposure timing is improved.

Detailed examination of the exposure pulse was undertaken to determine time of exposure based on rotational speed. Since the pulse shape is trapezoidal, the effective time of exposure can be taken as that at half-wave height, or as the average of the total time and the time at maximum amplitude. A photocell was placed behind a 0.1-inch-diameter aperture at the plane of the specimen and the exposure pulse was carefully studied at various rotational speeds. It was determined that the trapezoidal structure was very close to symmetrical (the opening time was slightly longer than the closing time) and that the time at half-wave height was  $88 \pm 2$  percent of the total time from first opening to full closure. This result was verified by examining the heating time, available from the oscillographic record of flux measurement with the SRI calorimeter (described below).

Careful measurement of the effective circular length of the aperture formed by the openings in the counter-rotating discs yielded a value of 6.24 inches. Since the locus of the aperture center is on a circle whose circumference is 40.0 inches, overall exposure time can be computed by the relationship  $9360/\text{rpm} = \text{msec}$ , and the effective exposure time in milliseconds is  $8240/\text{rpm}$ .



### C. Flux Measurement

The primary instrument for measuring incident flux is the SRI calorimeter described in Ref. 3; a detailed drawing of the device is shown in Fig. 5. Radiant energy passes through the aperture (about 0.1 inch in diameter) and falls on the sensing element, which is a blackened spherical copper segment. The calorimeter is used with the aperture occupying the same position as the front surface of a specimen. Radiation absorbed by the sensing element causes a temperature rise which is detected by a thermocouple at the back surface of the sensing element. The thermocouple signal is amplified and recorded on an oscillograph; absorbed flux is calculated from the rate of temperature rise, the area of the aperture, and the mass and heat capacity of the sensing element. Exposure time is limited so that the temperature rise does not exceed 50°C. Absorptivity of the blackened spherical segment is assumed to be 1.0 in calculating radiant flux incident on the propellant specimen.

An interlaboratory comparative calibration of calorimeters was recently undertaken to provide confidence in arc image furnace flux measurement. These efforts were coordinated by the Naval Ordnance Test Station; results are reported in Ref. 4. Comparison of the SRI calorimeter with one which was presumed to have a known absorptivity indicated that the effective absorptivity of the SRI calorimeter at that time had been about 0.88. The receiving surface of our calorimeter was later (May 29, 1965) carefully blackened with acetylene black from a carbide lamp; increased absorbed flux measurements indicated a previous absorptivity of about 0.83. Since that time we have blackened the surface twice and no indication was found that the absorptivity had degraded during the program.

An asymptotic calorimeter (manufactured by Hy-Cal Engineering Corp.), similar in design to one described by Gardon,<sup>5</sup> was procured for use on the BuWeps-sponsored program.<sup>2</sup> Initial comparisons with the SRI calorimeter appeared to yield close agreement. The original coating supplied with the Hy-Cal instrument degraded in a relatively

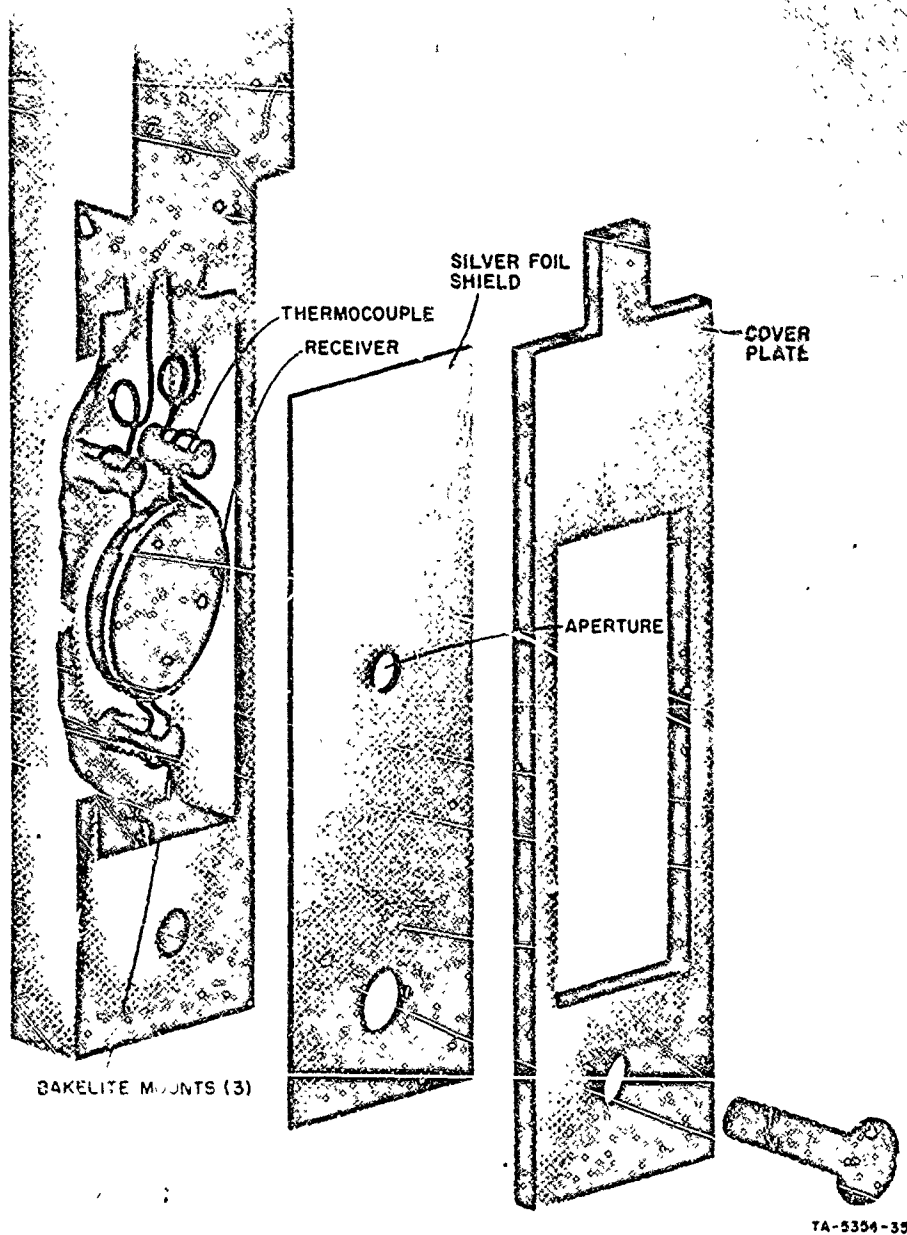


FIG. 5 SRI CALORIMETER FOR FLUX MEASUREMENT

short time and was removed; acetylene black from a carbide lamp was reapplied to the sensing surface routinely during the program. The Hy-Cal instrument is shown in Fig. 6 before and after blackening. The ignition bomb was modified to accommodate the Hy-Cal calorimeter, enabling flux measurements to be made readily during a series of tests. Since the asymptotic calorimeter is a total radiation device, its output can be recorded directly on a 10-mv potentiometer over any period of time as long as the maximum allowable flux is not exceeded.

Figure 7 is a photograph of the ignition bomb showing the Hy-Cal calorimeter in its stand-by position. Before a flux measurement is made, the Teflon storage plug is removed and the calorimeter head is inserted in its place. The Pyrex tube normally used for ignition tests is replaced with a half-tube to enable flux measurement at the plane of the specimen face.

Although the asymptotic calorimeter is fundamentally an easier instrument to use than the SRI calorimeter, it is not a primary standard. Thus, it must be calibrated against a known standard in order to determine its sensitivity. Furthermore, in the calibration procedure undertaken by the manufacturer, which is a sequence involving the use of a previously calibrated reference standard, calibration can only be accomplished up to a flux of about  $55 \text{ cal/cm}^2\text{-sec}$ , even though the calibration curve supplied with the instrument may be extrapolated to as high a flux as  $275 \text{ cal/cm}^2\text{-sec}$ .

Our original plan was to establish a calibrating factor between the SRI and Hy-Cal instruments and then to make routine use of the Hy-Cal instrument; the SRI calorimeter, which is a primary instrument, would then only be used for an occasional check. Unfortunately, the Hy-Cal calorimeter originally procured was defective; original difficulties with coatings and recalibration merged into the first signs of faulty operation, so that these first signs were not fully recognized at the time of their occurrence. The instrument was returned to the manufacturer and was replaced by another calorimeter with a maximum allowable flux of about  $135 \text{ cal/cm}^2\text{-sec}$  and a two-fold

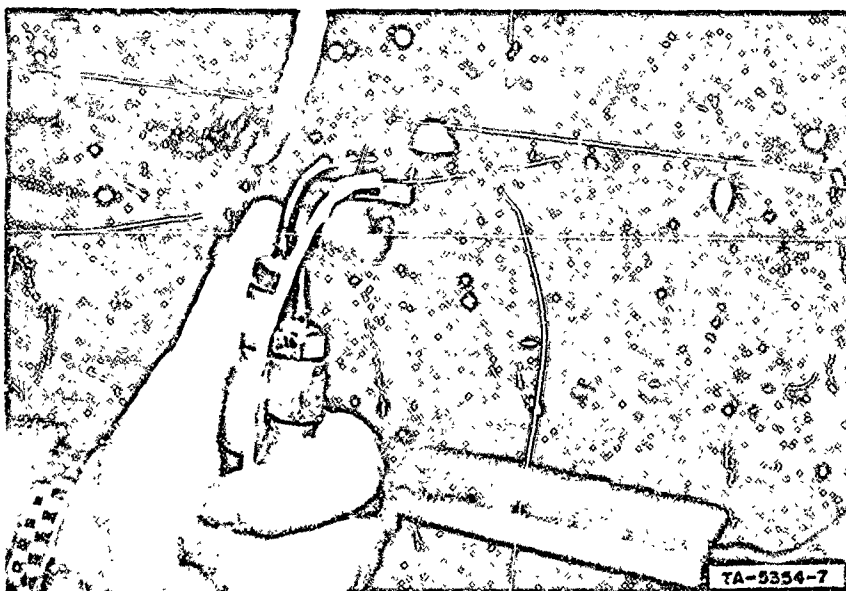
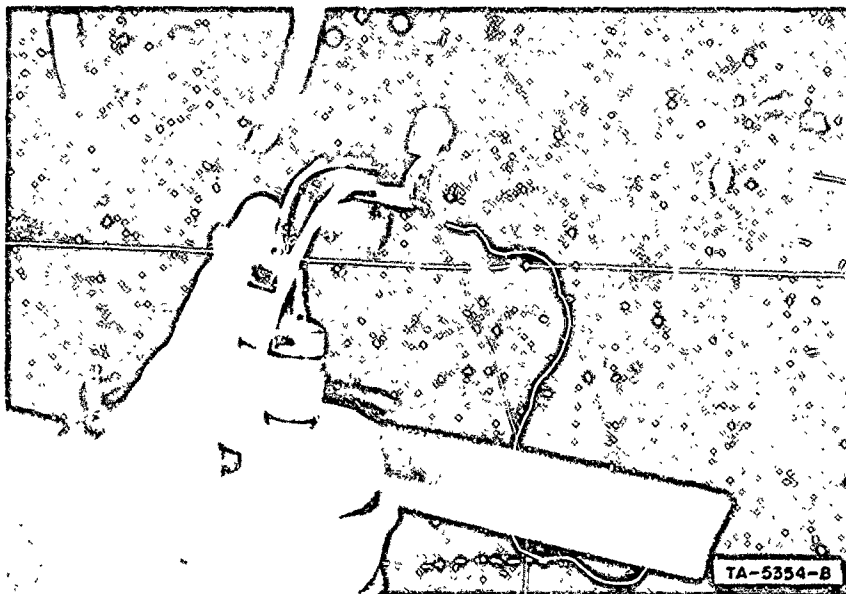


FIG. 6 HY-CAL CALORIMETER BEFORE AND AFTER BLACKENING

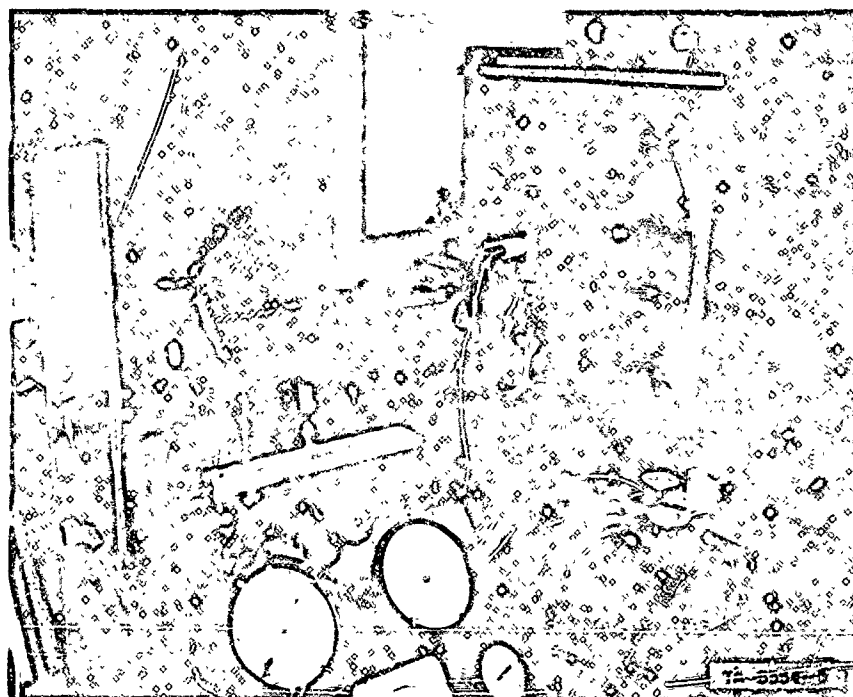


FIG. 7 IGNITION BOMB WITH HY-CAL CALORIMETER  
IN STAND-BY POSITION

increase in sensitivity. The replacement calorimeter was requested in an uncoated condition for application of acetylene-black during use.

During the program, time was lost due to investigations of coatings, comparisons between calorimeters, and recalibration. Use of the SRI calorimeter, which is more time-consuming, was more extensive than had been planned, but unfortunately not as extensive as we now realize it should have been. Resolution of experimental results required considerable examination of the records from both this program and the one sponsored by BuWeps.<sup>2</sup> Detailed evaluation of the probable sensitivity of the original Hy-Cal instrument during periods of change was required. In resolving the test data measurements of flux with the SRI calorimeter were considered to be correct. Sensitivities of the original Hy-Cal calorimeter ranged from that specified to the final values prior to return to the manufacturer; these sensitivities (25.5 to about 15 cal/cm<sup>2</sup>-sec per millivolt) increased with time but not in a regular manner. The sensitivity of the replacement calorimeter was about 15 percent lower than that specified upon receipt, but during the first three weeks of use it increased to the specified value. It apparently stabilized at that time and continued to operate satisfactorily for the remainder of the program.

#### D. Attenuation of Flux

To make ignition time measurements at various levels of flux, it was necessary to provide means for graded flux attenuation. Only those methods which do not modify the profile of the focal volume were considered acceptable. Thus, previously used methods such as apertures at the secondary image or vertical masks at the secondary mirror were discarded. The following is a list of methods developed and used during the course of the program:

1. Clear Pyrex plates or screens of various open areas placed between the shutter and the ignition bomb (Fig. 7)
2. Screens of about 70-, 50-, and 35-percent open area placed over the secondary mirror (Fig. 8).

3. A curtain consisting of bead-chains suspended at intervals from an extendible coil spring and placed between the shutter and the ignition bomb, for wide variability of flux densities.

These methods were used in various combinations to achieve the several flux levels desired. For example, a large-mesh, 70-percent open-area screen placed over the secondary mirror provided an incident flux of about  $70 \text{ cal/cm}^2\text{-sec}$ ; similarly, testing at about 7 to 12  $\text{cal/cm}^2\text{-sec}$  required the use of a combination of a small-mesh screen at the secondary mirror, a screen between the shutter and the bomb, and the bead-chain curtain, to select the desired level of flux.

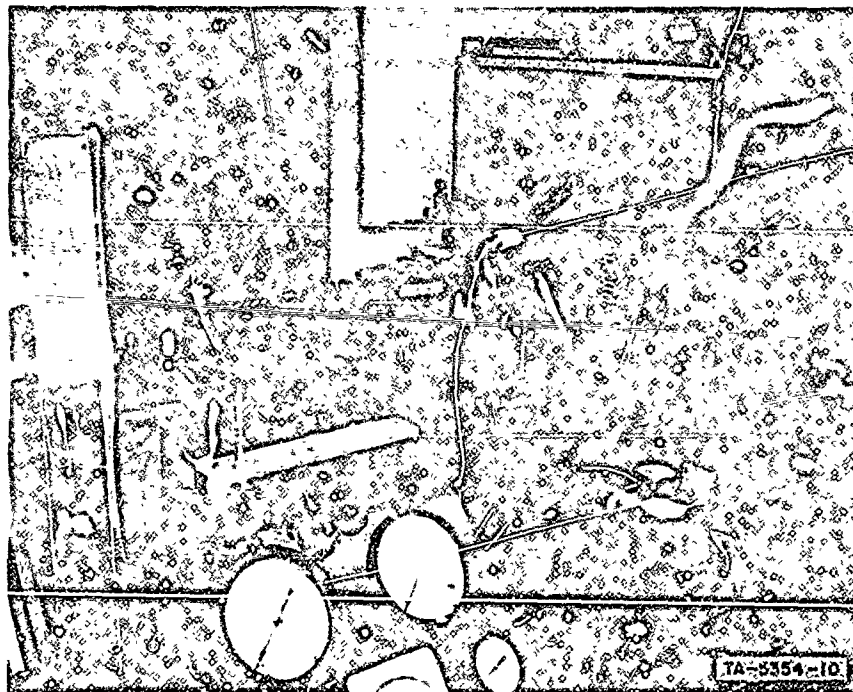


FIG. 8 TWO POSITIONS FOR PLACEMENT OF FLUX-ATTENUATING SCREENS

### III EXPERIMENTAL PROGRAM

The design of our experimental program was guided by the desire to establish interrelationships among ignition characteristics and compositional factors, and to examine the validity of the various suggested ignition theories. Our original intent was to collect extensive data on many operational or development-stage propellants, with auxiliary information being obtained from studies of model compositions prepared at the Institute. However, since the model compositions appeared to cover the range of compositional factors so well, we devoted the major part of the study to their characterization. We believe that considerably more information was gained by emphasizing the work on the model compositions than could have been secured by following the proposed plan of characterizing 15 operational propellants with uncontrolled compositional variations.

We spent considerable time in modifying the arc image furnace, in developing and evaluating flux measurement and attenuation methods, and in determining shutter timing characteristics. Some of this work, because of the calorimeter difficulties described above, continued into the ignition study phase. As a result, data were difficult to resolve and there is still some question as to the complete validity of some of the earlier data. Nevertheless, the test data are for the most part consistent and amenable to analysis.

#### A. Experimental Method

The ignition time,  $\tau$ , reported here is the time of exposure to radiant flux required to effect ignition, or to initiate a state of sustained combustion. We choose to determine this time, or ignition threshold, by using go/no-go tests, in which successive specimens are exposed to energy pulses of known durations and successful or unsuccessful ignition is recorded in each case. Depending upon test conditions, ignition may occur at the time of energy flux cessation or at some delayed time thereafter. The reproducibility of the delay



time has been found to be poor.<sup>1</sup> Because of this and because of the instrumentation difficulties involved, we chose not to measure the delay time during this program.

In other programs,<sup>6,7</sup> ignition times were measured by maintaining sustainer radiation and determining the time to first light. It has been suggested that this is the manner in which rocket motors are ignited. Anderson and Beyer<sup>6</sup> found the method to be cumbersome and unreliable. More important, we believe that data obtained in such a manner can be misleading in attempting to gain an understanding of the ignition process and its underlying mechanisms. The low flux radiation furnace used at the Institute<sup>8</sup> and at the University of Utah<sup>9</sup> are examples of continuous energy application through the ignition phase. Results of both studies demonstrate the inadequacy of the method. Institute results obtained at 14.7 psia were found to compare favorably with arc image furnace data taken at 300 psia.<sup>8</sup> Baer and Ryan<sup>9</sup> found no pressure dependency over a range of pressures from 0.18 to 11 atmospheres. Such experiments do not allow for surface gasification and flame under conditions which would not favor sustained combustion had the application of energy ceased upon first light. Both programs yielded test results typical of pressure-insensitive ignition behavior, as would normally occur at high pressures.

Further illustration of this objection to the method of sustained radiation and light detection can be found in the results of the Interlaboratory Solid Propellant Ignition Exchange Program.<sup>10</sup> When the test data were plotted as  $\log \tau$  versus  $\log$  flux, results of those facilities using light detection methods agreed among themselves and showed no pressure effects, while go/no-go test results agreed relatively well but did demonstrate considerable influence of pressure.

A variation of the ignition threshold method was introduced during this program. Previous determinations at low pressures, where ignition times became long, were beset by wide go/no-go limits. This was to be expected because in that region the curve approaches an infinite

slope. Therefore, to obtain a smaller bandwidth of data, thresholds were obtained in the low-pressure region by holding time constant and finding the go/no-go limits of pressure.

All tests were conducted in a nitrogen gas environment. In each case, the ignition bomb was flushed with nitrogen prior to pressurization. At pressures below atmospheric, although pressure was maintained by bleeding air into a surge tank connected to the ignition bomb, the diffusion path was sufficiently long that no air would be expected in the region of the test specimen. Little or no gas flowed in the region of the specimen during a test; pressure control was maintained by gas bled into or out of the system at the surge tank.

Test specimens were discs of material, 0.3 inch in diameter by about 0.1 inch thick. The specimens were prepared by cutting with a cork-borer from a sheet of the propellant prepared with a sharp microtome knife. The cut surface was not as smooth as that obtainable by machining, but was sufficiently uniform to maintain reproducibility of test results.

#### B. Materials

The materials studied in this program included five operational propellant types, seven model compositions prepared at the Institute, and four pressed pellet compositions. The operational propellants were Aerojet-General Corporation formulations; these had been in magazine storage at the Institute for periods ranging from one to five years. Brief descriptions of these compositions are as follows:

ANB 3066	aluminized polybutadiene composition
ANB 3105	aluminized polybutadiene composition
ANP 2677	polyurethane composition
ANP 2639AF	aluminized polyurethane composition
ANP 2969KH-1	aluminized polyurethane composition

The model compositions consisted of an epoxy anhydride cured PBAN binder, ammonium perchlorate, and additives as shown in Table I. The ammonium perchlorate used was supplied by Pennsalt Corporation and was processed to a bimodal blend of 70 percent unground - 30 percent ground material; the average particle size of the unground material was about 180 microns, that of the ground material was about 11 microns. Strand burning rates for these model compositions are shown in Fig. 9. The pressed pellet compositions were representative of the solids of the variable catalyst systems, i.e. PBAN-254, PBAN-259, PBAN-260, and PBAN-264.

Table I  
MODEL PROPELLANT COMPOSITIONS

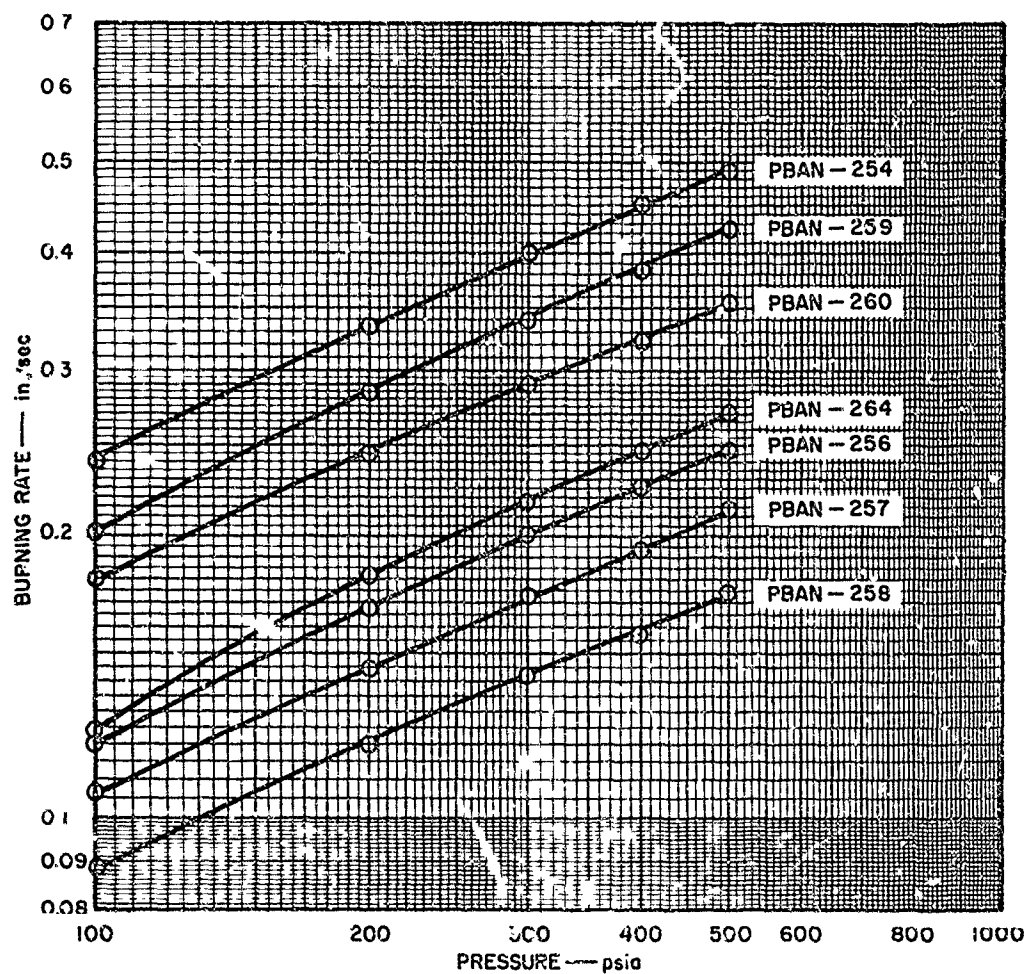
Identification	Wt % AP	Wt % Thermax	Wt % CuO2O2
PBAN - 258	70.00	1.00	--
PBAN - 257	75.00	1.00	--
PBAN - 256	80.00	1.00	--
PBAN - 264	85.00	1.00	--
PBAN - 260	85.00	1.00	0.20
PBAN - 259	85.00	1.00	0.50
PBAN - 254	85.00	1.00	1.00

### C. Test Results

All test results are shown in Tables II, III, and IV. Test conditions (i.e., flux and pressure) are included in the tabulations. Results of many of the repeated tests are also shown; however, those repeated tests made for verification at nearly the same time as the first test are not reported. Results are reported as go/no-go limits of pressure or time. Statistical representation of these test results is impractical; we believe that plotting of the data limits provides

sufficient information as to their reliability or unreliability. Although no error analysis was attempted, if consideration of absolute values of absorbed flux is omitted, the accuracy of the measurements is assumed to be about  $\pm 5$  percent. A discussion of errors will be included in the final report of the BuWeps-sponsored program.<sup>2</sup>

Graphical representations of the data are presented in Figs. 10 - 27, inclusive. Depending upon the extent of the testing performed on each material, results are plotted as  $\log \tau$  versus  $\log \phi$  (where  $\tau$  and  $\phi$  are exposure time and energy flux, respectively) and as  $\log \tau$  versus  $\log$  absolute pressure. Only one pellet composition is reported graphically, since successful ignition was obtained only at high pressure and since a sufficient number of tests at varying flux was performed on only the one composition.



YB-5354-30

FIG. 9 BURNING RATES OF MODEL PROPELLANT COMPOSITIONS PREPARED BY SRI PROPULSION LABORATORY

Table II  
RESULTS OF TESTS OF MODEL PROPELLANT COMPOSITIONS

COMPOSITION	PRESSURE, psia	FLUX, cal/cm <sup>2</sup> -sec	EXPOSURE TIME, msec	COMPOSITION	PRESSURE, psia	FLUX, cal/cm <sup>2</sup> -sec	EXPOSURE TIME, msec
PBAN-254	14.7	115	9.9- 9.2	PBAN-264 (cont'd)	14.7	21	165- 155
	14.7	81	15.8-14.5		14.7	11	445- 435
	14.7	58	23.5-22.2		14.7	8	1100-1030
	14.7	35	47-43.5		215	92	10.3- 9.2
	14.7	28	61-59.5		215	61	13.7-12.7
	14.7	22	103- 99		215	51	18.3-16.5
	14.7	11	390- 410		215	32	31.7-28.4
	14.7	8	1060-1000		215	13	235- 210
	215	91	4.8- 4.4		515	72	11.3-10.3
	215	65	8.3- 7.5		215	72	11.3-10.6
	215	38	18.7-17.5		45	72	19.6-18.7
	215	25	45.8-43.3		6.8-6.6	72	103
	215	12	420- 410		5.6-5.3	70	235
	215	7	1270-1180		665	46	21.1-20.1
	215	62	8.5- 8.3		515	46	21.1-20.1
	215	12	435- 410		315	51	18.7-17.5
	715	46	13.7-11.8		115	46	21.7-20.1
	515	46	13.7-11.8		14.7	46	41-37.5
	315	46	13.7-11.8		6.8-6.0	46	103
	115	46	13.7-11.8		5.8-5.6	46	165
	14.7	46	22.8-20.6		5.1-4.9	46	235
	7.3-6.8	46	53		4.6-4.4	46	410
	6.6-6.3	46	103	PBAN-256	415	60	17.2-15.8
	6.3-5.8	46	206		215	60	17.2-17.0
	4.4-3.9	46	410		165	60	18.7-18.3
	4.4-4.1	46	550		115	60	21.1-20.6
PBAN-259	14.7	72	18.7-17.2		55	60	24.2-23.6
	4.9-4.6	72	206		14.7	60	40- 38
	715	64	11.8-10.3		5.8-5.4	60	106
	715	56	15.0-12.9		4.4-4.1	60	133
	315	65	10.8- 8.2		3.9-3.6	60	235
	215	56	15.8-12.3		3.4-3.1	60	410
	215	66	10.3- 9.2		3.1-2.9	60	635
	115	65	11.0- 9.7		115	70	11.4-10.3
	65	65	11.0- 9.7		14.7	70	36- 33
	14.7	67	22-20.6		215	65	11.8-10.3
	8.3-7.8	56	53	PBAN-257	715	60	20.6-19.8
	6.8-6.3	56	103		615	60	20.6-19.8
PBAN-260	6.8-6.3	56	206		315	60	24.2-23.5
	5.8-5.4	56	410		215	60	24.2-23.5
	4.9-4.4	56	550		115	60	24.2-23.5
	5.4-5.1	67	825		65	60	33-30.5
	14.7	140	17.9-17.2		14.7	60	47.3-45.6
	14.7	121	17.9-17.2		7.8-7.3	60	68.5
	14.7	80	23.5-21.5		5.8-4.9	60	82.5
	14.7	70	26.6-23.6		4.9-3.9	60	165
	14.7	62	31.5-27.5		3.9-3.4	60	410
	14.7	42	44.5-42.5		3.4-2.4	60	825
	14.7	27	69- 75	PBAN-258	315	69	12.2-11.5
	14.7	13	232- 229		115	71	13.3-12.9
	14.7	7	825- 820		14.7	71	57- 53
	215	121	5.1- 4.9		215	137	6.9- 6.6
	215	80	7.1- 6.6		215	96	11.8-11.1
	215	62	11.8-10.3		215	63	16.8-15.8
	215	62	13.1-12.1		215	40	21.7-20.6
	215	42	19.6-18.7		215	27	38.3-37.4
	215	27	55-48.5		215	12	211- 206
	215	14	206- 201		215	7	1180-1030
PBAN-264	215	7	785- 750	PBAN-258	865	60	28.4-27.5
	715	46	22.3-20.6		515	60	30-29.5
	315	46	19.2-18.2		415	60	33-29.5
	215	46	20.6-19.9		215	60	30.5-29.5
	115	46	19.9-19.4		115	60	28.4-26.6
	65	46	21.1-20.6		65	60	29.5-27.5
	14.7	56	31.6-30.5		35	57	41- 39
	7.3-7.6	67	53		14.7	60	57- 55
	6.6-6.3	46	103		7.35	60	137- 127
	5.8-5.6	67	206		5.8-4.9	57	410
	4.9-4.6	56	410		3.9-2.9	57	825
	215	65	11.8-10.3	PBAN-254	315	69	22.9-22.6
	115	63	13.7-11.8		115	70	29.4-27.5
	14.7	115	19.6-18.7		14.7	71	55- 53
PBAN-264	14.7	81	29.4-27.5				
	14.7	58	43.4-40.2				
	14.7	35	78.5- 75				
	14.7	28	90.5-88.5				

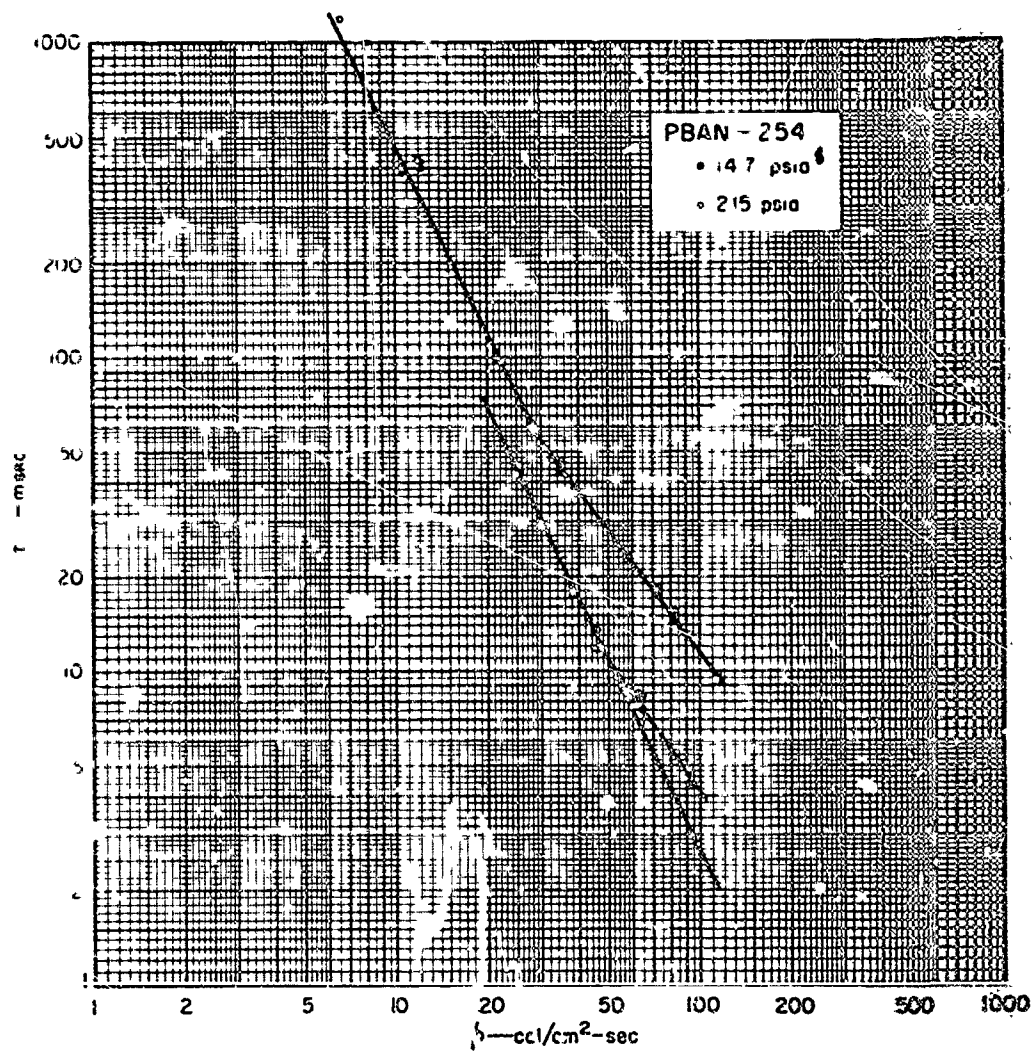
Table III  
RESULTS OF TESTS OF PRESSED PELLETS

COMPOSITION	PRESSURE, psia	FLUX, cal/cm <sup>2</sup> -sec	EXPOSURE TIME, msec	REMARKS
Pellet No. 3 (PBAN-254)	815	81	8.2- 7.5	
	815	69	16- 15	
	815	36	33-27.5	
	815	23	137- 118	
	615	64	16.5-15.8	
	215	64	217- 211	ablation
	215	20	282- 250	ablation
	75	64	--	non-ignition
Pellet No. 4 (PBAN-259)	815	69	18.7-18.3	
	815	35	41- 37	
	815	22	91- 75	
	615	64	32- 29	
	215	64	--	heavy ablation
	215	20	--	heavy ablation
	75	64	--	non-ignition
Pellet No. 5 (PBAN-260)	815	69	33-27.5	ablation
	815	35	--	heavy ablation
	615	62	--	non-ignition
	215	62	--	non-ignition
	215	18	--	non-ignition
Pellet No. 6 (PBAN-264)	815	68	20.5-16.5	
	815	35	--	heavy ablation
	615	62	--	non-ignition
	215	18	--	non-ignition

Table IV  
RESULTS OF TESTS OF PROPELLANT COMPOSITIONS

COMPOSITION	PRESSURE, psia	FLUX, cal/cm <sup>2</sup> -sec	EXPOSURE TIME, msec
ANB-3066	615	68	16.6-14.7
	415	68	16.5-14.7
	265	69	20- 19
	215	68	23.5-21.5
	165	69	26.5- 25
	115	58	41- 33
	65	72	29.5-27.2
	35	69	72- 66
	14.7	72	82.5- 75
	7.3- 7.1	72	103
	4.8- 4.5	67	275
	215	131	6.4- 5.5
	215	91	12.1-11.8
	215	67	24-20.5
	215	40	46- 41
	215	25	82- 75
	215	23	87- 82.5
	215	12	915- 825
	215	11	680- 550
	35	130	22.9-21.7
	35	91	35- 33
	35	58	48.5-43.5
	35	41	87-82.5
	35	24	242- 206
	35	11	1370-1180
	50	62	48.5- 41
	40	62	51.5- 46
ANB-3105	665	73	16.5-15.7
	565	73	19.5- 15
	215	73	25-23.5
	115	73	27.5-23.5
	55	62	33-31.6
	35	62	40- 39
	14.7	70	59-48.5
	5.1- 4.8	70	103
	4.1- 3.9	70	206
	3.9- 3.6	70	410
	3.4- 3.1	70	825
ANP-2677	415	70	15.8-15.2
	215	70	15.8-15.2
	115	71	19.2-17.9
	65	71	24.2-21.6
	14.7	70	69- 64
	7.6- 7.3	72	103
	4.6- 4.3	72	206
	3.9- 3.6	72	410
ANP-2639 AF	715	70	12.7-11.8
	515	70	14.5-13.7
	315	70	20.6-18.7
	115	62	23-21.5
	35	70	59- 50
	14.7	70	295- 285
	13.3- 13	70	206
	11.7-11.5	70	410
ANP-2969 KH-1	415	70	24.2-23.2
	215	70	24.2-23.2
	115	70	28.4-27.5
	65	70	46- 41
	65	71	43- 39
	35	68	55- 53
	14.7	71	non-ignition
	11.7-11.5	70	825





TB-2334-19

FIG. 10 DEPENDENCE OF EXPOSURE TIME ON FLUX: PBAN-254

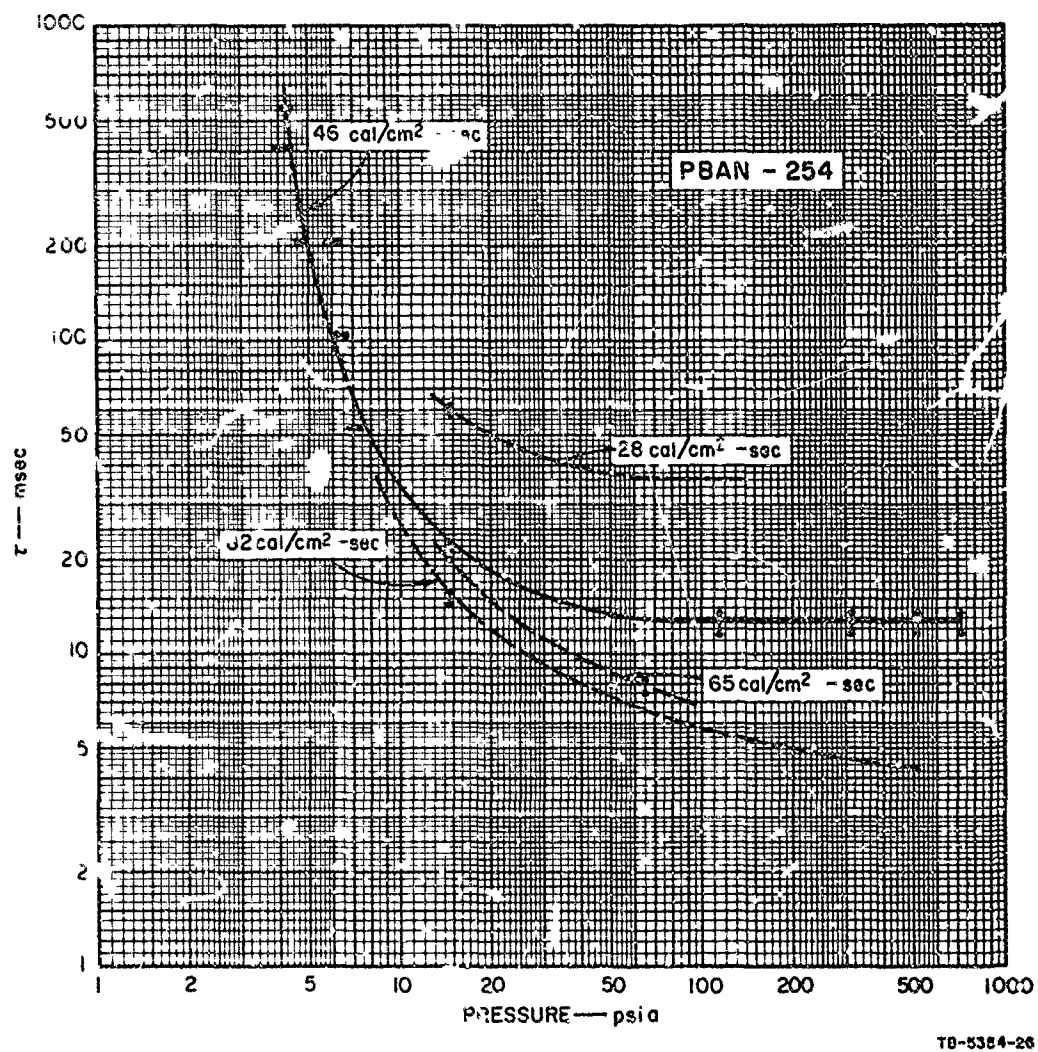
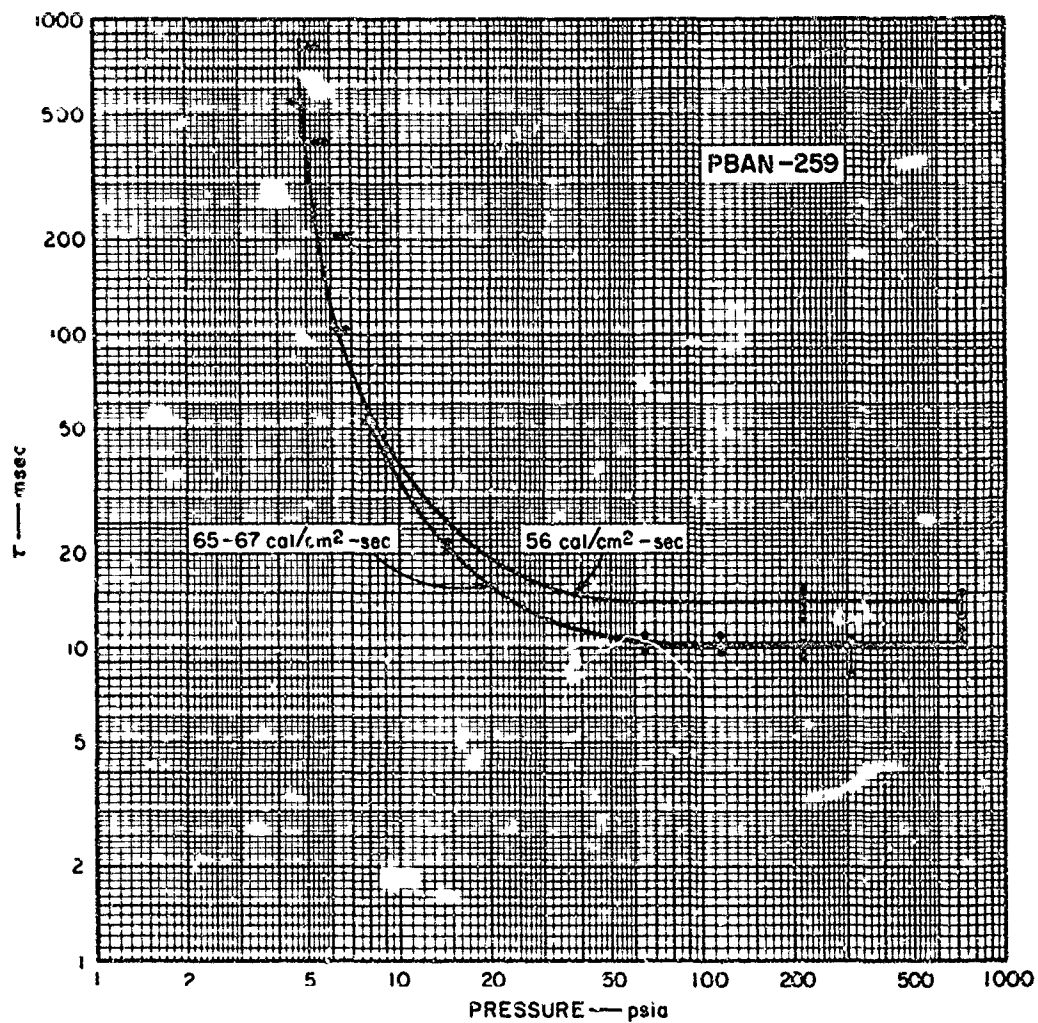
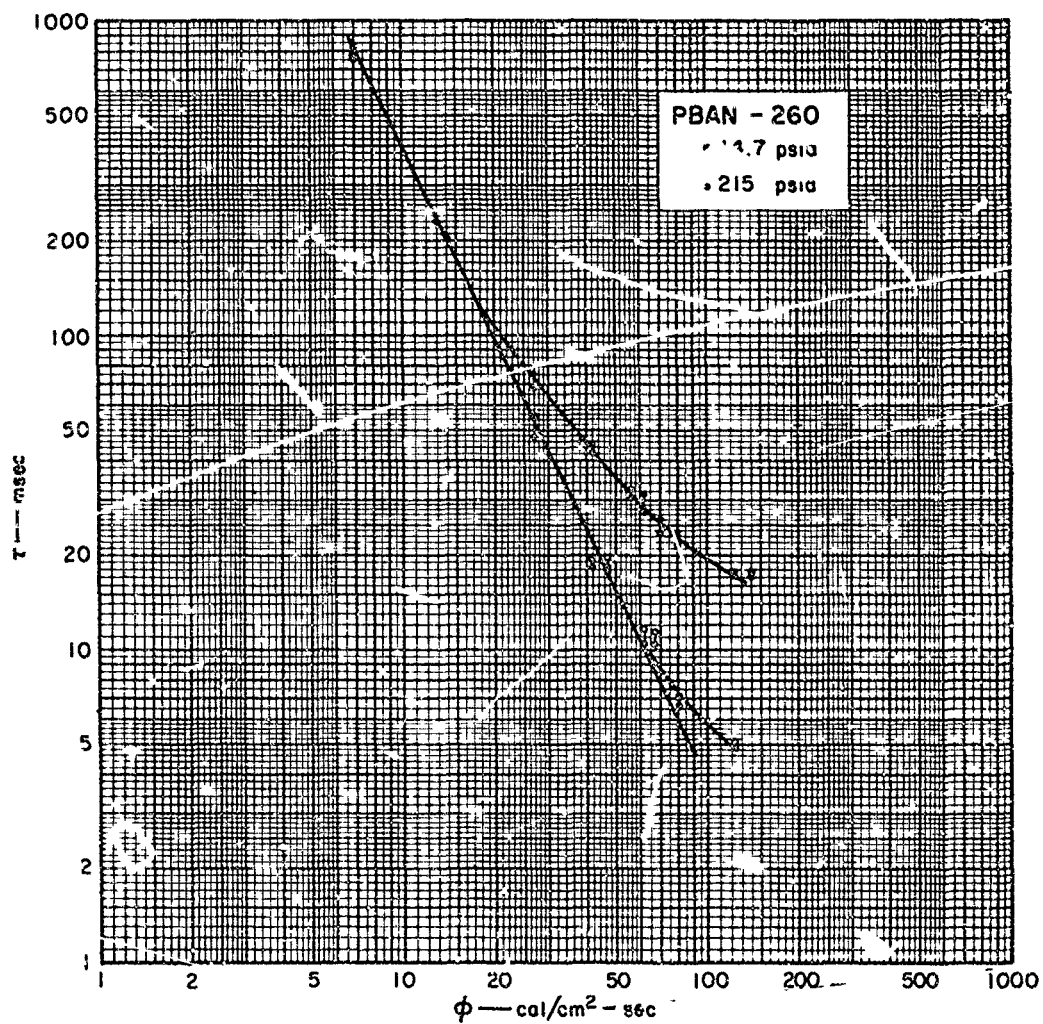


FIG. 11 DEPENDENCE OF EXPOSURE TIME ON PRESSURE: PBAN-254



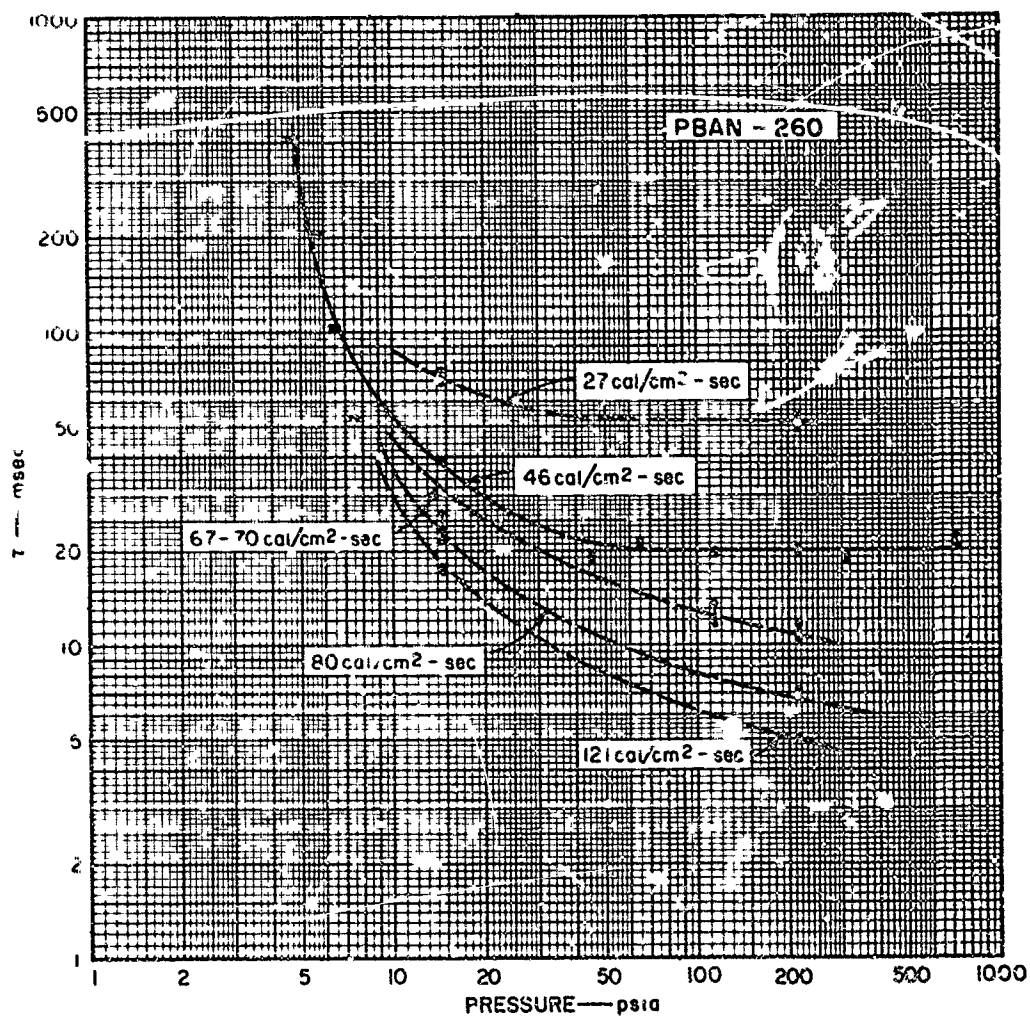
78-5354-27

FIG. 12 DEPENDENCE OF EXPOSURE TIME ON PRESSURE: PBAN-259



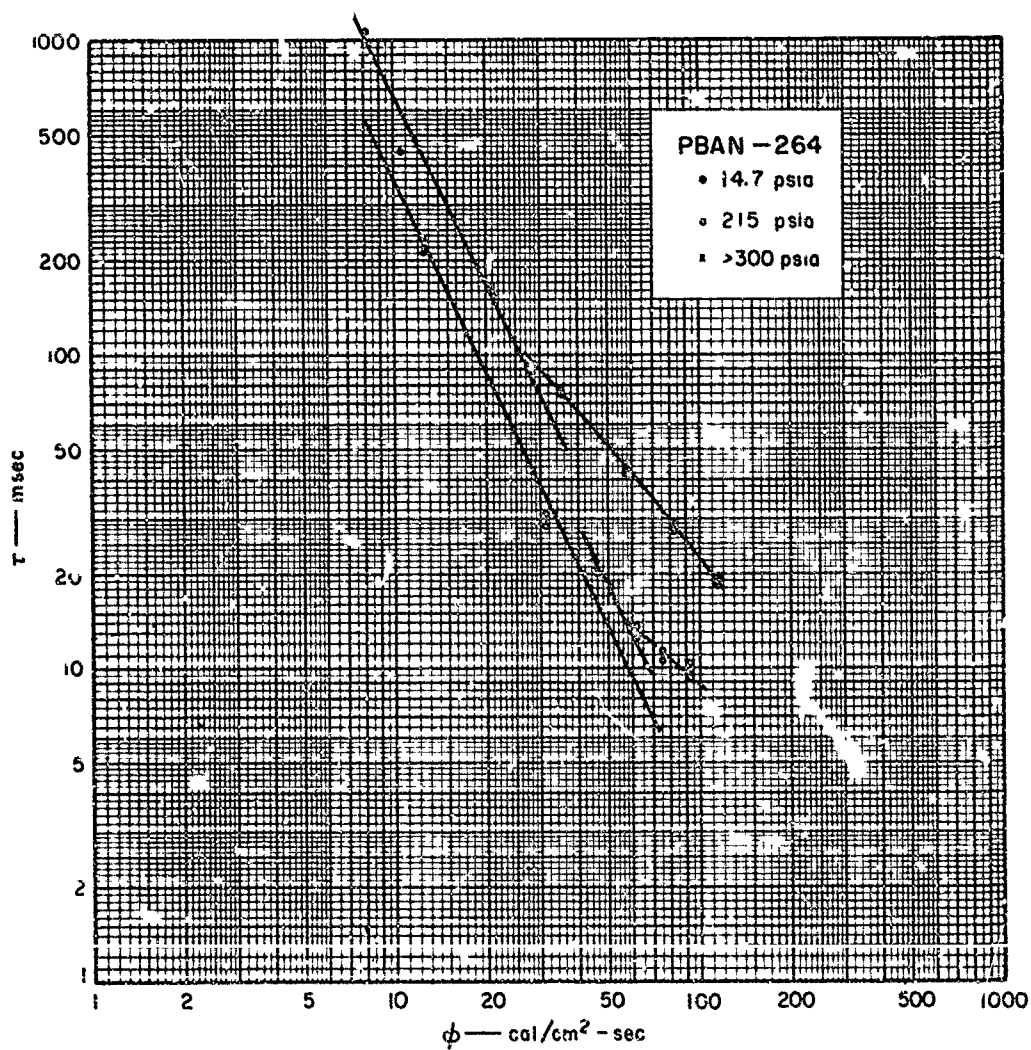
TB-5354-20

FIG. 13 DEPENDENCE OF EXPOSURE TIME ON FLUX: PBAN-260



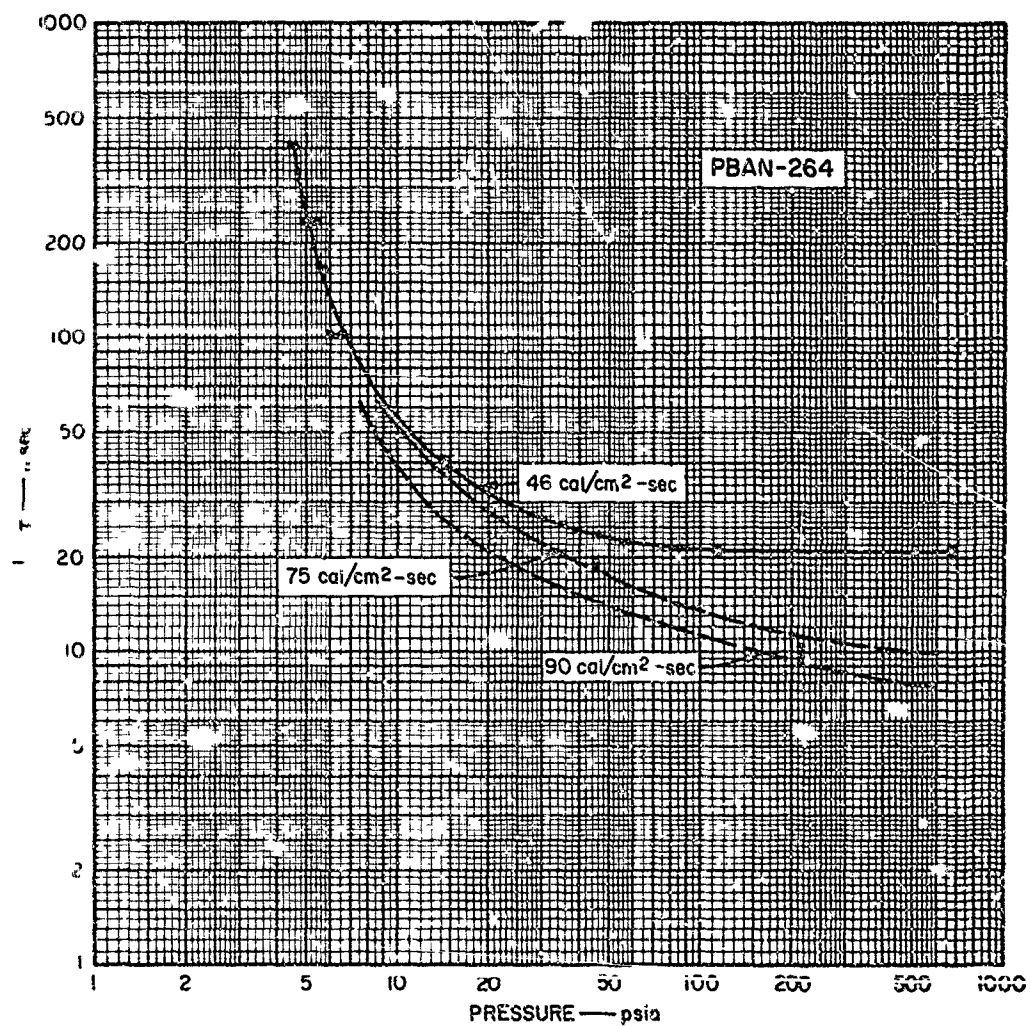
YB-5354-23

FIG. 14 DEPENDENCE OF EXPOSURE TIME ON PRESSURE: PBAN-260



T6-3354-18

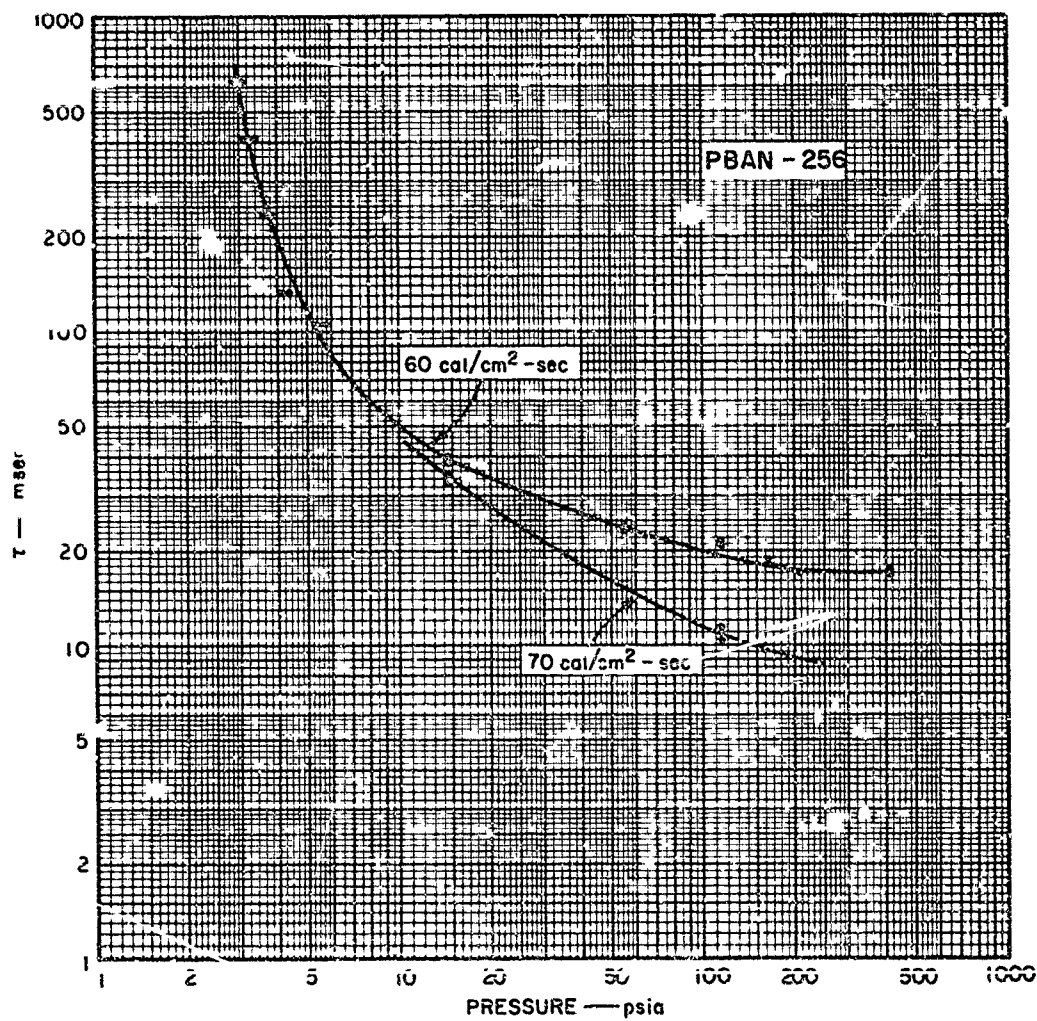
FIG. 15 DEPENDENCE OF EXPOSURE TIME ON FLUX: PBAN-264



TB-5354-28

FIG. 16 DEPENDENCE OF EXPOSURE TIME ON PRESSURE: PBAN-264

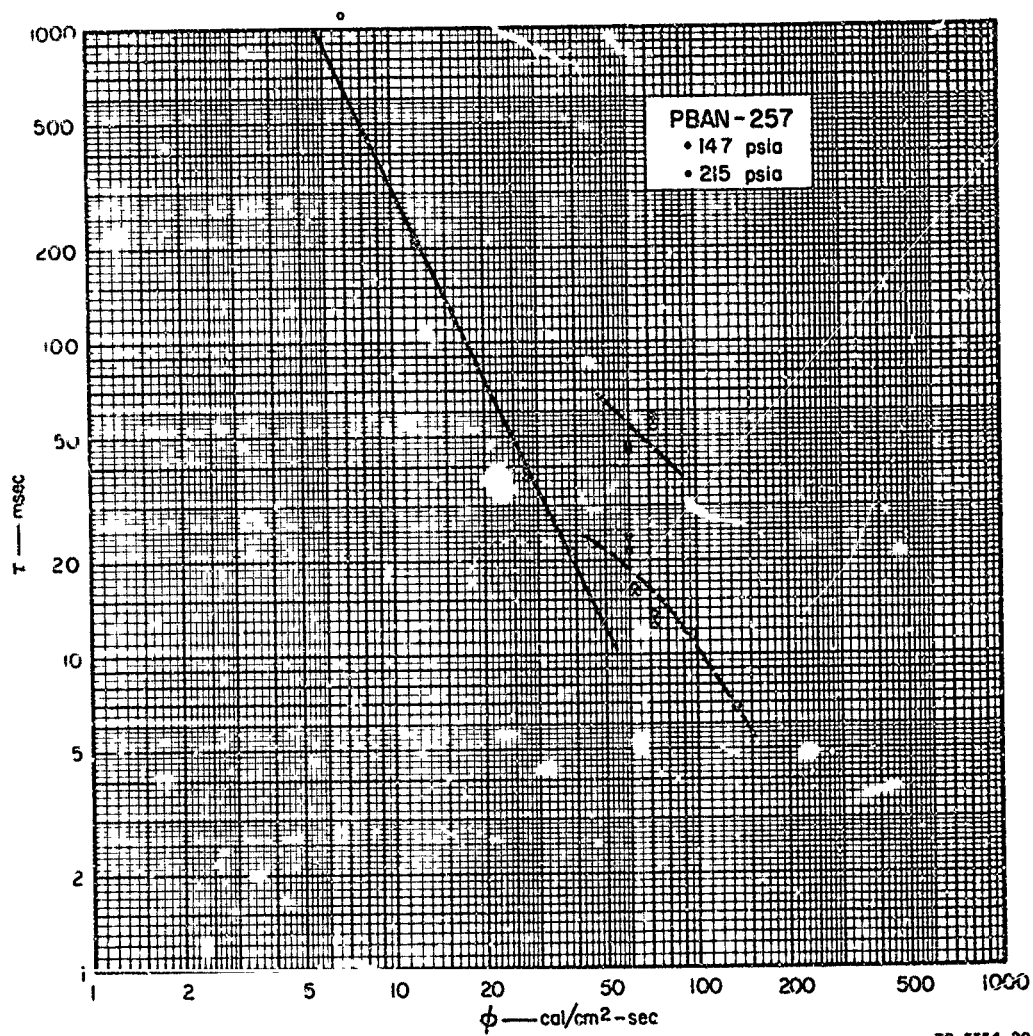




TB-5384-17

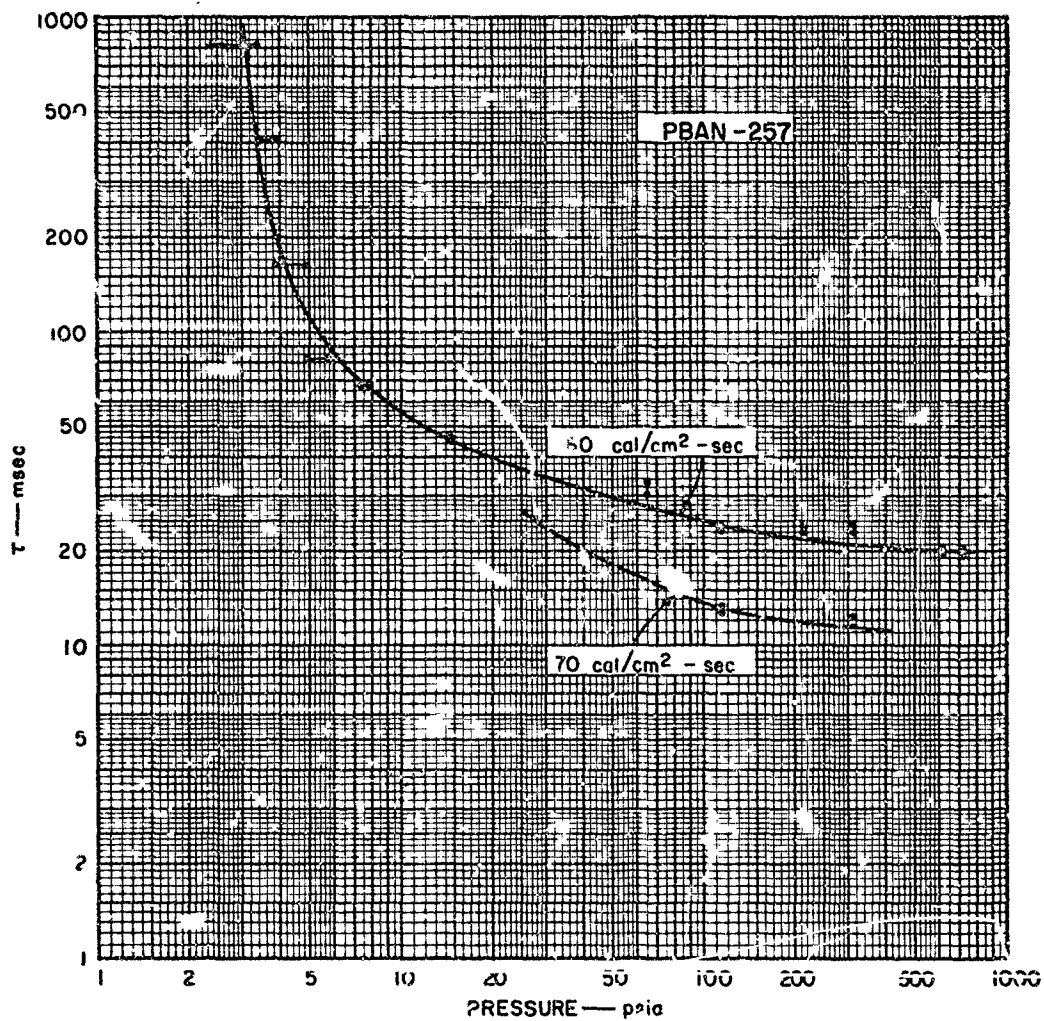
FIG. 17 DEPENDENCE OF EXPOSURE TIME ON PRESSURE: PBAN-256





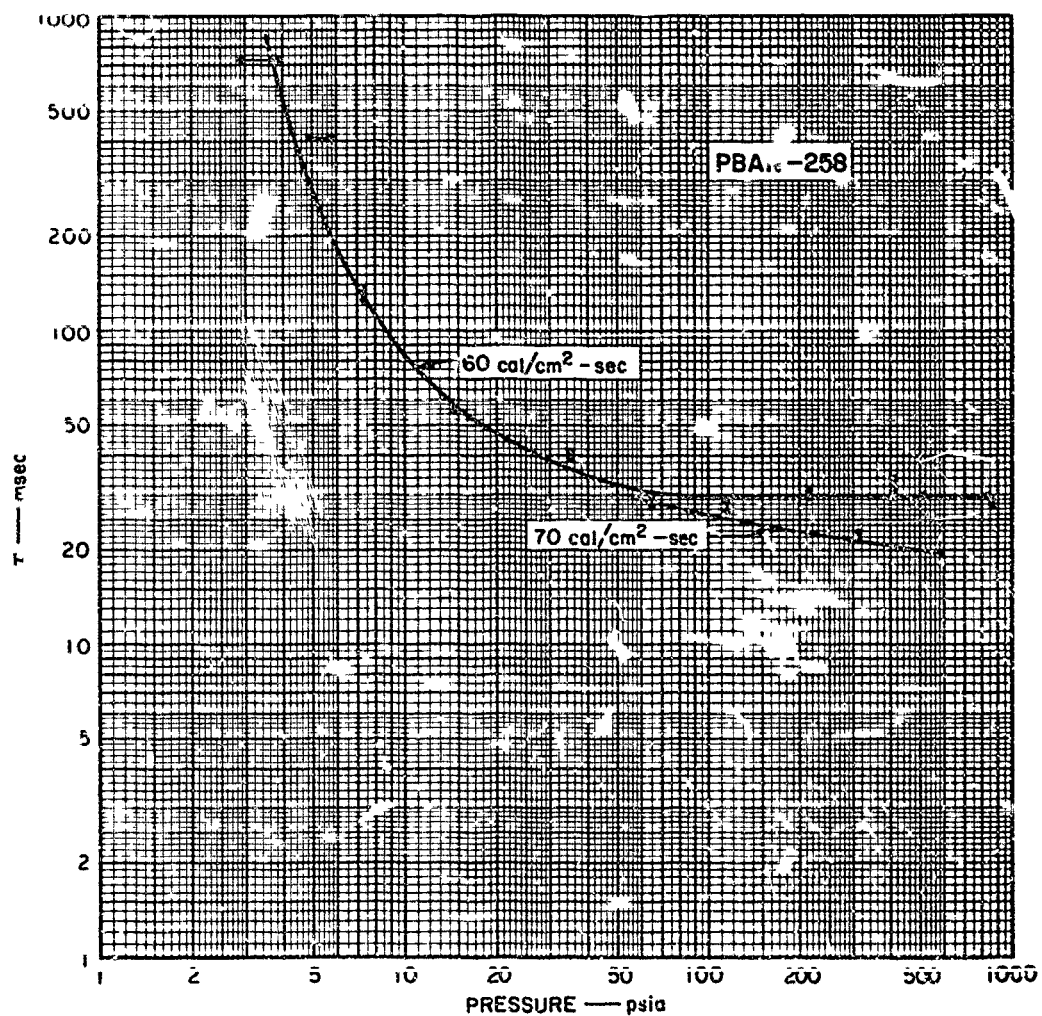
TB-5354-29

FIG. 18 DEPENDENCE OF EXPOSURE TIME ON FLUX: PBAN-257



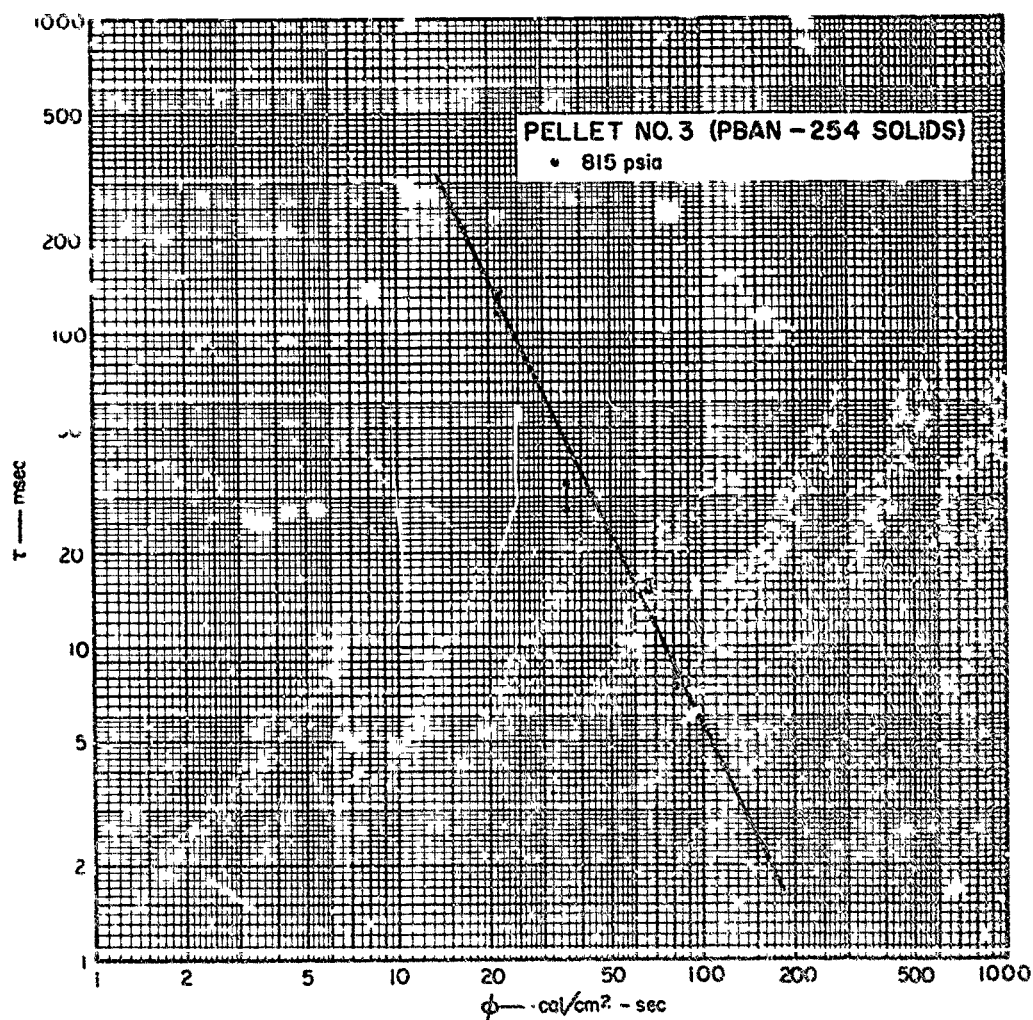
TB-5354-13

FIG. 19 DEPENDENCE OF EXPOSURE TIME ON PRESSURE: PBAN-257



TB-5354-19

FIG. 20 DEPENDENCE OF EXPOSURE TIME ON PRESSURE: PBAN-258



TB-5354-22

FIG. 21 DEPENDENCE OF EXPOSURE TIME ON FLUX: PELLETT NO. 3  
(PBAN-254 solids)

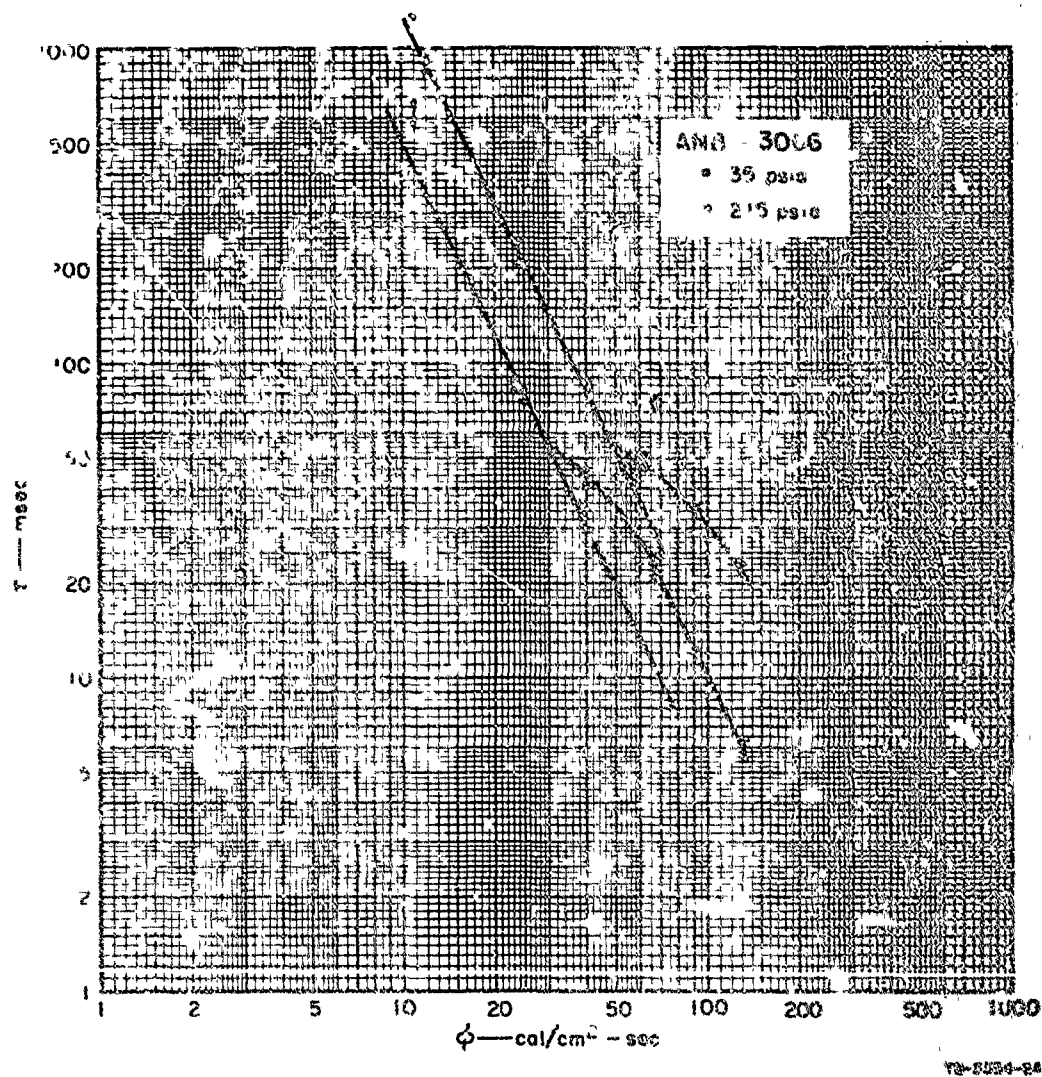
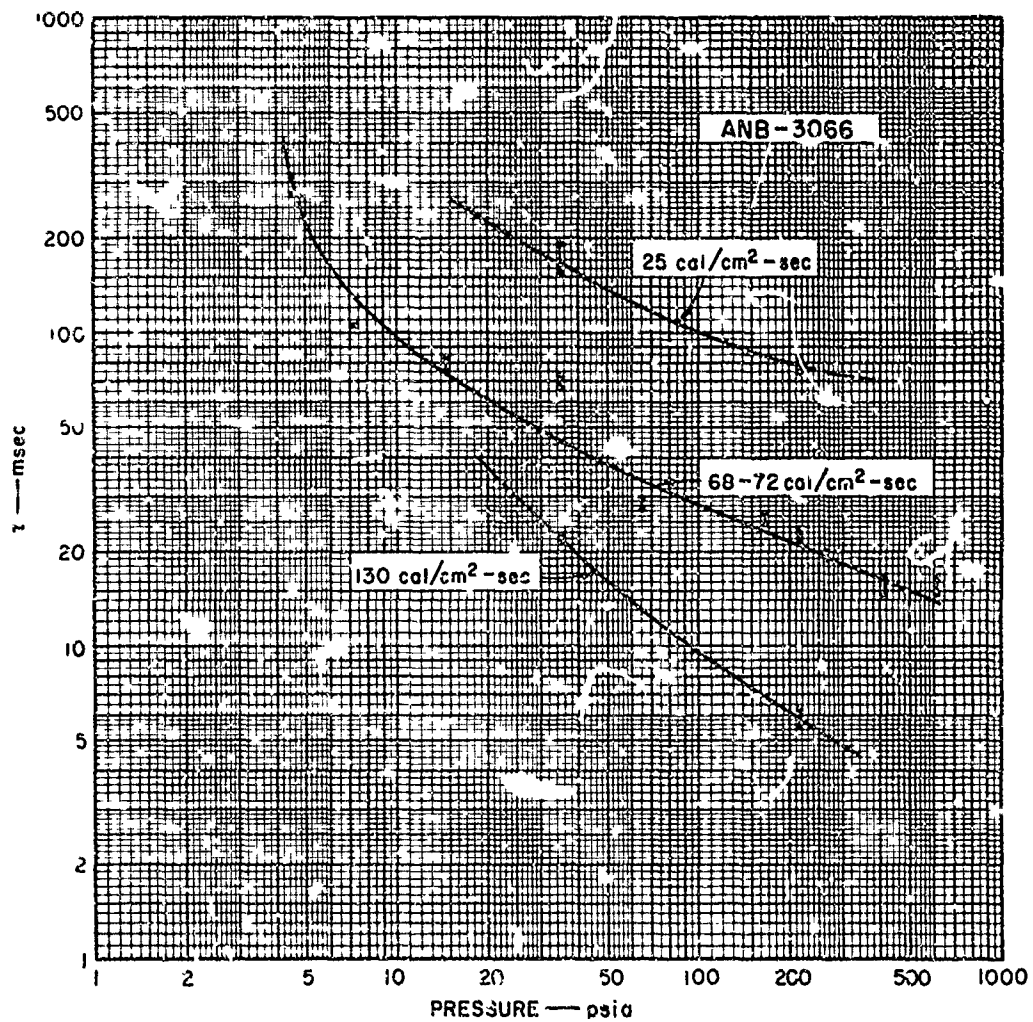
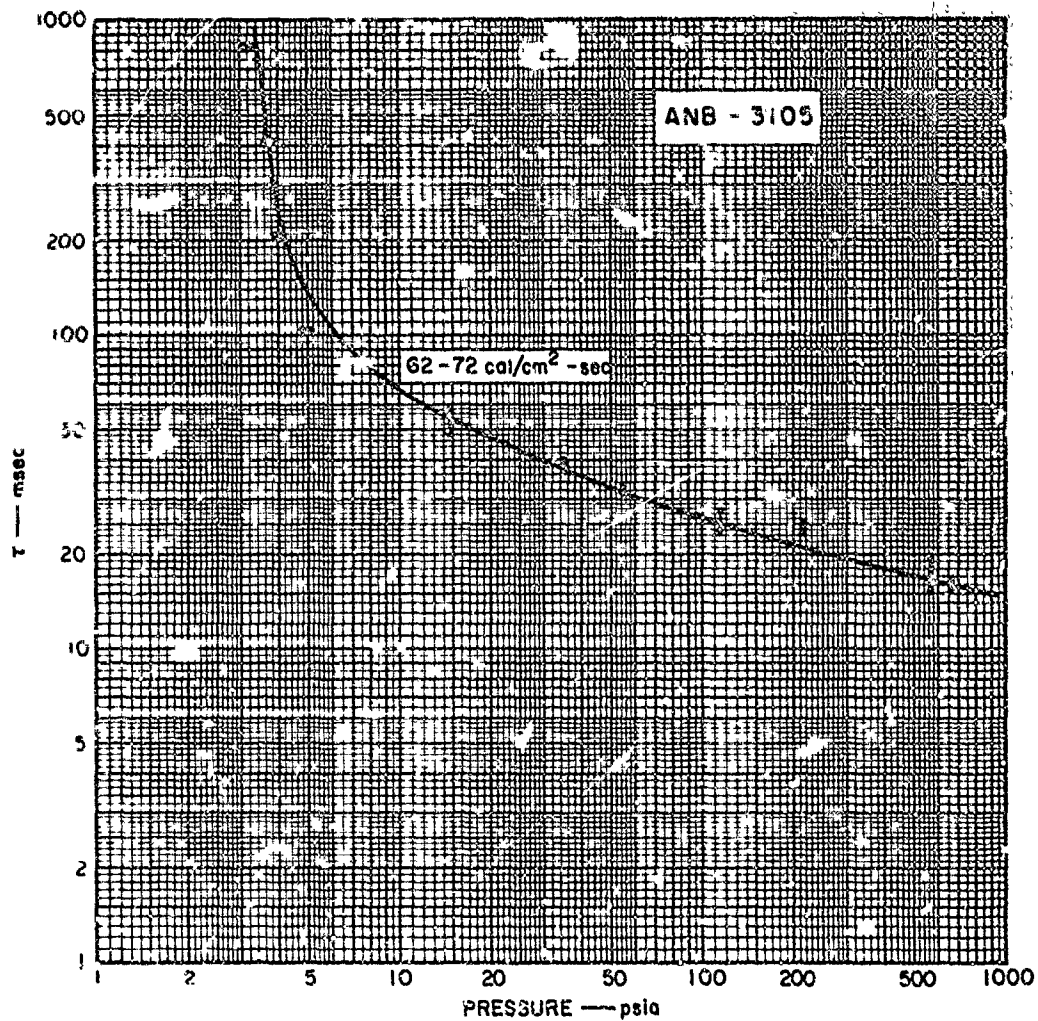


FIG. 22 DEPENDENCE OF EXPOSURE TIME ON FLUX: ANB-3006



TB-5314-25

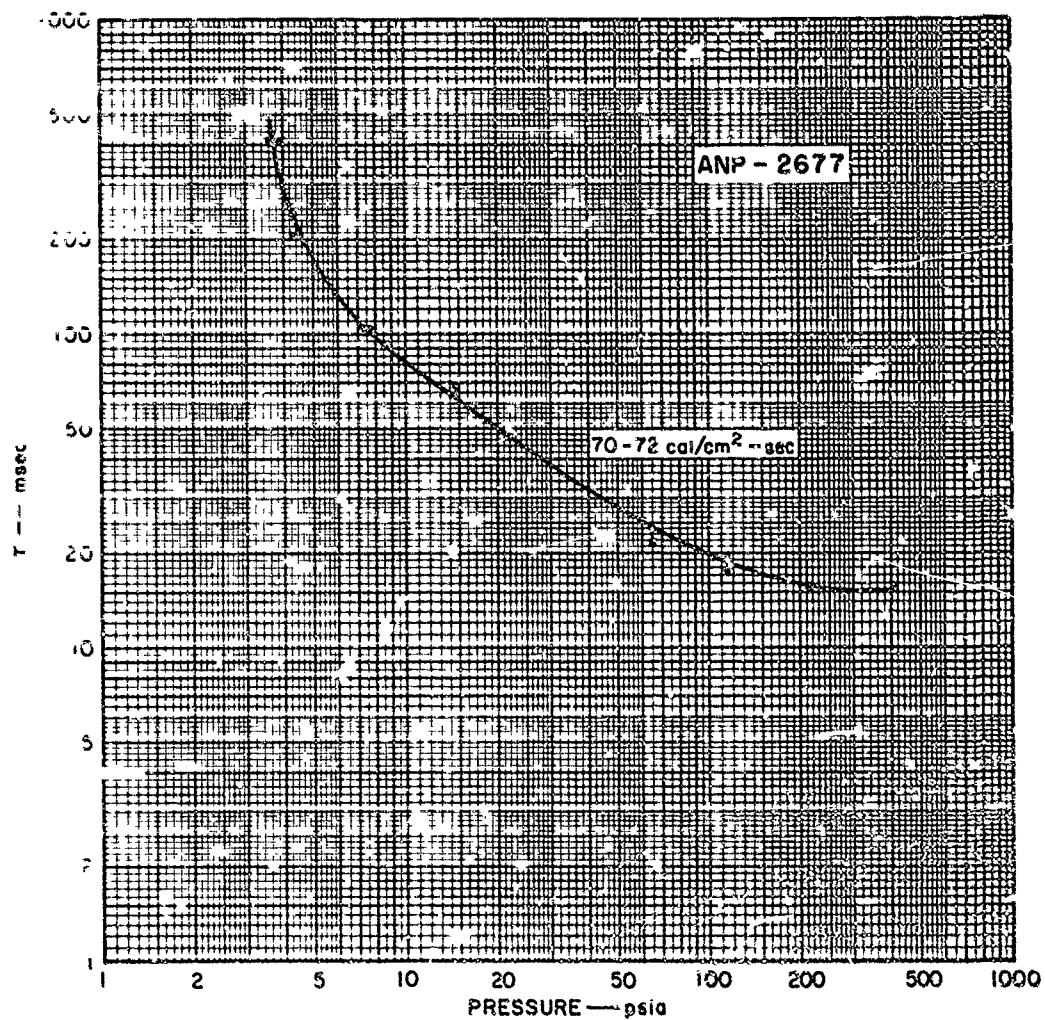
FIG. 23 DEPENDENCE OF EXPOSURE TIME ON PRESSURE: ANB-3066



TB-5554-21

FIG. 24 DEPENDENCE OF EXPOSURE TIME ON PRESSURE: ANB-3105

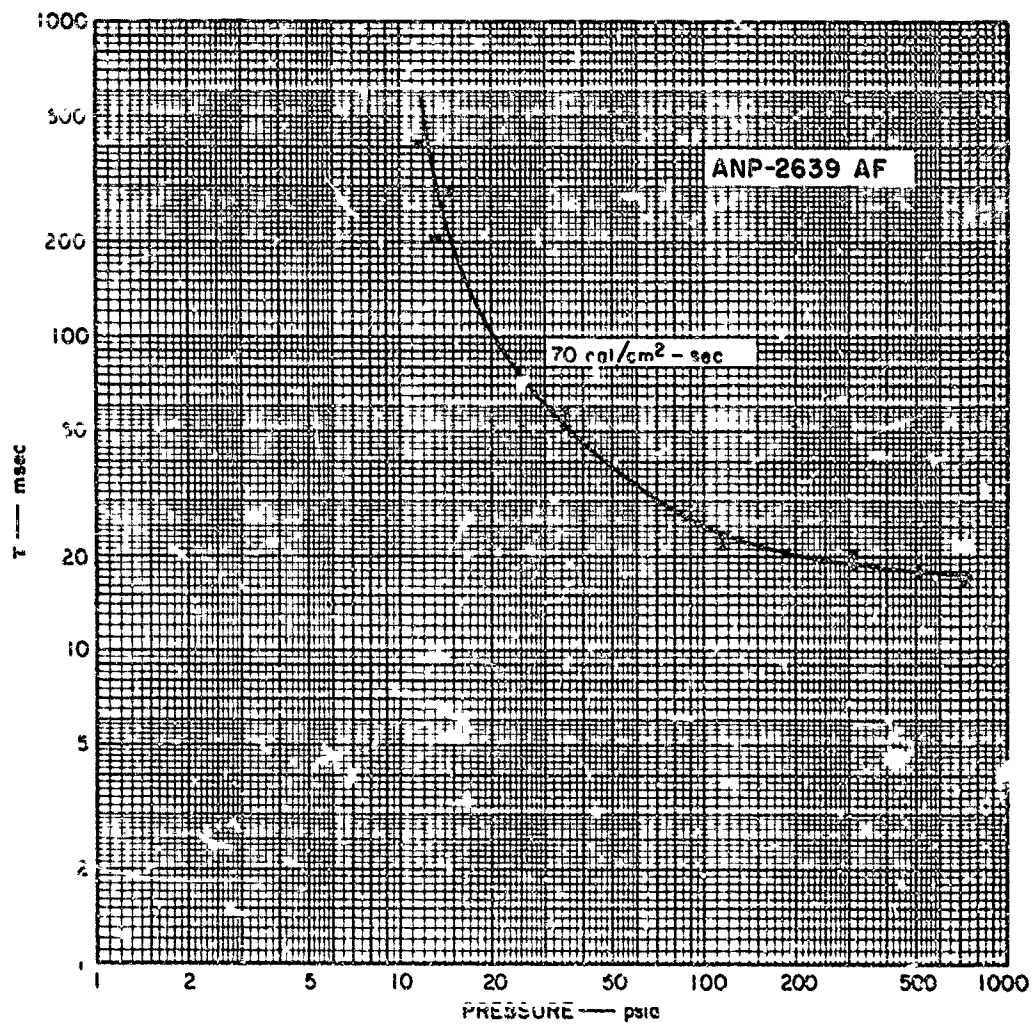




78-5384-18

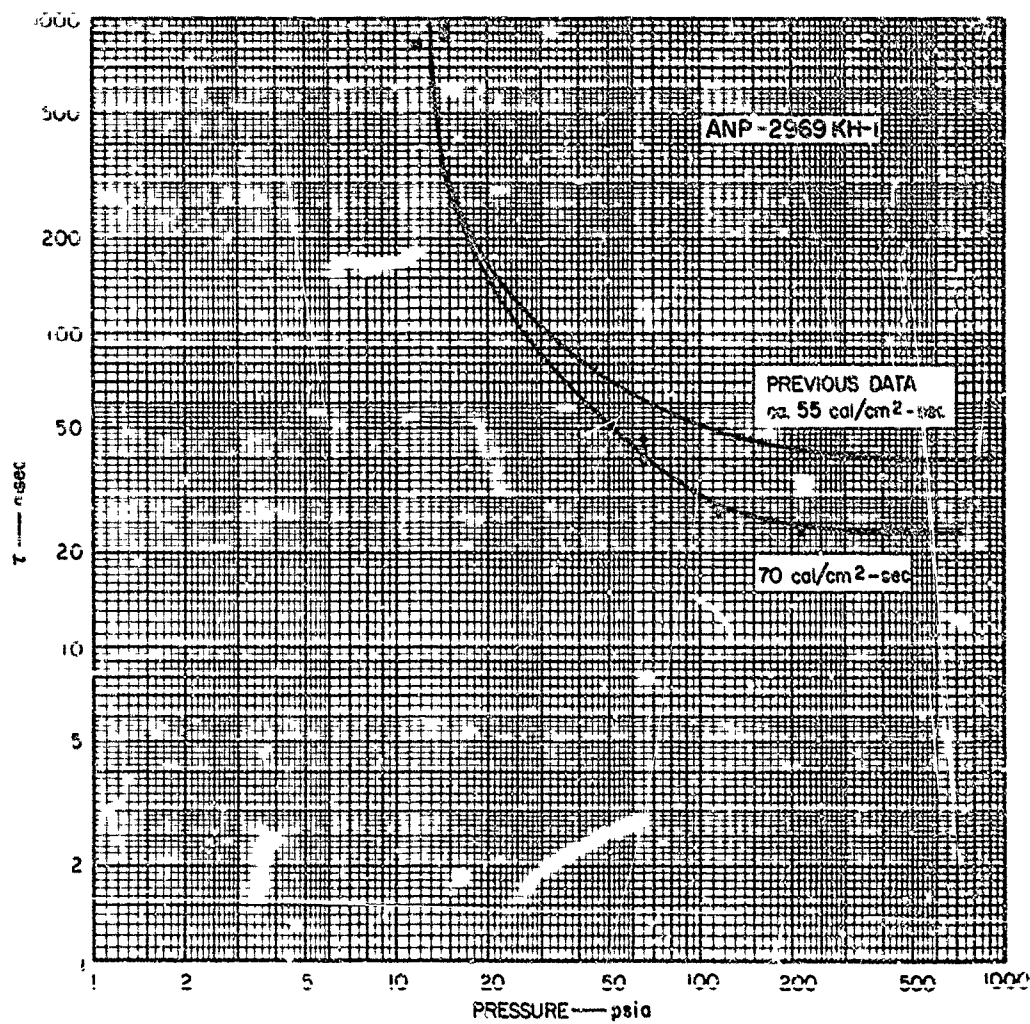
FIG. 25 DEPENDENCE OF EXPOSURE TIME ON PRESSURE: ANP-2677





TC-6384-14

FIG. 26 DEPENDENCE OF EXPOSURE TIME ON PRESSURE: ANP-2639AF



FB-5354-22

FIG. 27 DEPENDENCE OF EXPOSURE TIME ON PRESSURE: ANP-2969KH-1

#### IV DATA ANALYSIS

##### A. Discussion of Test Results

Test data are graphically represented as  $\log \tau$  versus  $\log P$  and as  $\log \tau$  versus  $\log \phi$ . The pressure effect on exposure time for ignition,  $\tau$ , is most readily observable from plots of  $\log \tau$  versus  $\log P$  when the ranges of time and pressure are large. In general, these curves are bounded by an asymptote of infinite slope at the extreme of low pressure and by an asymptote of zero slope at high pressures. These boundary conditions represent the minimum pressure for ignition, and the pressure-independent exposure time for ignition, respectively.

The representation of flux dependence (i.e.  $\log \tau$  versus  $\log \phi$ ) results from the solution of the transient heating problem, which relates surface temperature, time, and energy flux for a semi-infinite slab of inert, opaque material under conditions of constant heat flux at the surface. If the test data for one composition fall on a line of slope equal to -2.0 on a plot of  $\log \tau$  versus  $\log \phi$ , and if there is no chemical reaction, ignition is characterized by a constant surface temperature which is independent of flux. Other commonly used plotting methods depict the same results; a constant surface temperature is represented by a  $\log \tau^{1/2}$  versus  $\log \phi$  slope of -1.0 and by a  $\log (\phi\tau)$  versus  $\log \phi$  slope of -1.0.

The go/no-go limits of all data were plotted, rather than the average values of time or pressure, to demonstrate the data spread. As mentioned above, statistical handling of the data was not practical, since the number of tests was usually not sufficient to apply a Bruceton or similar analysis. However, under the same conditions of flux and pressure, the repeatability of the test results is excellent and we have a high degree of confidence in individual data points as presented.

We observe from the  $\log \tau - \log \phi$  plots that the data are rather well fit by a line of slope equal to  $-2.0$  up to a particular value of flux, at which point the data begin to deviate toward larger values of time. Thus it appears that, at least up to a certain characteristic value of flux, it is valid to assume a constant value of surface temperature at ignition, independent of flux.

Because of calorimeter difficulties, some doubt exists as to the incident flux associated with some of the data obtained early in the program, and certain aspects of the results are questionable. In particular, there may be a discrepancy in the locations of the lines of slope equal to  $-2.0$  on the  $\log \tau - \log \phi$  plots for different pressures. From Figs. 10, 15, and 22 it is apparent that, prior to deviation from the line of constant slope, the data are fit by two parallel lines; i.e., the ignition temperature is not the same at the two pressures.

However, the data for PBAN-260 in Fig. 13 indicate that the same surface temperature characterizes ignition at both pressures. These latter data are not likely to be unique, because of the composition of the propellant, and would be expected to be valid because, in this case, tests were performed alternately between the two pressures as flux was increased. In the cases of PBAN-254 and PBAN-264, data at the two pressures were obtained at times separated by about six weeks. On the other hand, the data for ANB-3066 (Fig. 22) were obtained on two consecutive days and separation between pressures appears to be valid.

In addition, the ANB-3066 data indicate that the constant surface temperature criterion is also met at 215 psia in the high flux region. This and the other similar observations noted above lead to the possibility that there may in fact be two or more regions of pressure-independent behavior, characterized by different ignition temperatures. Recognizing that the ignition process is composed of complex interactions among such phenomena as heat flow, mass transfer, homogeneous and

heterogeneous chemical reactions, and phase change, we should not avoid consideration of different regions of behavior at different pressures and energy fluxes.

Examination of the  $\log \tau - \log \phi$  plots yields the following general ignition characteristics:

1. From low flux levels up to a certain characteristic value ( $20 \text{ cal/cm}^2\text{-sec}$  and higher for these data), ignition appears to occur at a constant surface temperature.
2. As pressure is increased, the region of deviation from the line of  $-2.0$  slope occurs at shorter times.
3. When ignition time becomes pressure-independent at a specified flux level, that time is characterized by the line of  $-2.0$  slope.
4. Increasing pressure tends to suppress deviation from the line of  $-2.0$  slope; deviation from that line is eliminated in a pressure-independent regime.

Characteristics observed from the  $\log \tau - \log P$  plots include:

1. The general influence of pressure on exposure time is as described above--the  $\log \tau - \log P$  plots are curves bounded by an asymptote of infinite slope representing minimum pressure for ignition, and an asymptote of zero slope representing the pressure-independent regime.
2. The minimum pressure for ignition appears to be independent of flux in the range studied.
3. Pressure effects appear to be strongly influenced by flux, in that pressure independence is achieved at lower pressures as flux is reduced. For example, in the data for PBAN-260 (Fig. 14), exposure time is independent of pressure above about 40 psia at  $27 \text{ cal/cm}^2\text{-sec}$  and 70 psia at  $46 \text{ cal/cm}^2\text{-sec}$ ; pressure independence is not yet achieved at 215 psia at  $70 \text{ cal/cm}^2\text{-sec}$ .

It is obvious that the ignition characteristics inferred from the two types of data representation are interrelated and merely demonstrate the same behavior patterns from two different viewpoints. Using the example of PBAN-260, one can trace along the  $46 \text{ cal/cm}^2\text{-sec}$  curve of Fig. 14 from 14.7 to about 70 psia to reach the pressure-independent

region; in Fig. 13, one might then expect to start on the 14.7-psia curve at  $46 \text{ cal/cm}^2\text{-sec}$  and move downward vertically by successive tests at increasing pressure until, at about 70 psia, the line of -2.0 slope is reached.

The general behavior of the model propellant systems is as described above, with differences due to compositional variation. Pellet ignition data, shown in Fig. 21 and Table III, are not as complete as was desired. Sufficient data for plotting  $\log \tau$  versus  $\log \phi$  were obtained only on Composition No. 3; the others were successfully ignited only at 815 psia and only limited data were obtained over a range of flux. These pellets were difficult to ignite at lower pressures and demonstrated either large dependence on pressure or heavy ablation and nonignition.

The general behavior of the operational propellant compositions was similar to that of the model systems. Ignition data for ANB-3066 obtained at several fluxes were typical of those obtained for the model systems, with the possible exception that pressure dependence at 215 psia was demonstrated even at the lower flux levels. Accordingly, both ANB-3066 and ANB-3105 failed to achieve pressure independence at  $70 \text{ cal/cm}^2\text{-sec}$  when tested at pressures up to about 650 psia (Figs. 23 and 24). Even at a flux level of  $25 \text{ cal/cm}^2\text{-sec}$ , the ignition of ANB-3066 appears to be dependent upon pressure up to 215 psia. The polyurethane compositions are similarly pressure-dependent at  $70 \text{ cal/cm}^2\text{-sec}$  up to pressures in the range of 200 to 300 psia; ANP-2639 AF appears to exhibit pressure dependence even at the highest pressure tested, 715 psia.

#### B. Interrelationships among Compositional Factors and Ignition Characteristics

With this discussion as background, we can now examine the data for effects of compositional variations on ignition behavior. Prior to this program we had accumulated considerable data on operational propellants from several small test programs and attempted to achieve

correlation among compositional factors and ignition characteristics. There did appear to be a relationship between the stoichiometry (as represented by the ratio of weight percent AP to weight percent  $\text{CH}_2$ ) and the curvature of the  $\log \tau - \log P$  plots near one atmosphere. However, this finding was based on limited data and probably reflected only second order effects. In addition, with such a wide variation in composition differences, the chances of pin-pointing specific compositional effects were remote. At the start of this program, past data were reexamined; the task of obtaining sufficient data from studies of operational propellants to perform an adequate analysis appeared to be much too formidable. We therefore emphasized characterization of the ignition behavior of the model compositions which were detailed in Table I.

From the discussion presented above, we can consider specific ignition characteristics identifiable from the data. These include:

1. Minimum pressure for ignition
2. Exposure time (or ignitability level) in the pressure-dependent region
3. Pressure dependence as measured by the deviation from the line of -2.0 slope on the  $\log \tau - \log p$  plots.

We will discuss the effects of compositional factors on these ignition characteristics in the order listed.

First, we must make one general statement concerning rocket motor ignition. It is obvious from these data, as it has been since the pressure effect on ignitability was first noted, that ignition is most likely to be reliably accomplished if the ignition system is operative in the pressure-independent regime of the propellant. Thus, if the igniter supplies a short time pulse of high flux energy, the port pressure should be elevated to a sufficiently high pressure to ensure successful ignition in the time available. By continuing this reasoning, one can see that longer time exposures to energy at lower flux levels are likely to be generally successful and less

dependent on pressure. Although not a part of this program, past observations lead to the conclusion that ignition delay times are also reduced when ignition systems operate in the pressure independent region.

1. Minimum pressure for ignition. By examining the results of tests on the model propellant systems, we observe that in general there is little difference in the minimum pressure for ignition. The low-pressure asymptote for all four compositions with 85-percent ammonium perchlorate appears to be about 4 psia. Minimum pressures for the three compositions having increased binder contents appear to decrease to the range of about 2.5 to 3 psia; as binder content increases, the general level of required exposure time increases, and the low-pressure data become more difficult to determine. Thus it appears that the binder, which is the same in all the model compositions, is the factor most important to minimum pressure characteristics, and that ammonium perchlorate may tend to have an effect of raising this minimum.

Extending this observation to the operational propellants studied, we note that the two polybutadiene-type propellants (ANB-3066 and ANB-3105) exhibit minimum pressures of about 3 to 3.5 psia, and that two polyurethane propellants (ANP-2639AF and ANP-2969KH-1) have minimum pressures of about 10 to 12 psia. An exception appears to be the polyurethane propellant ANP-2677, which has a minimum pressure comparable to that of the polybutadiene types. The failure of ANP-2677 to fit the pattern may be related to the fact that it contains some potassium perchlorate or that the binder composition is such that it has a high decomposition temperature range.

It appears then that binder type (and presumably its pyrolysis and volatilization characteristics) is in fact a predominant factor in regard to minimum ignition pressure. The minimum pressure will depend upon the extent to which the pyrolysis and volatilization processes accompanying thermal decomposition divert energy from



the processes leading to ignition. The propellant whose binder is more difficult to decompose thermally or that decomposes at a higher temperature will exhibit a lower minimum pressure for ignition than the propellant whose binder is more readily decomposed. Polyurethanes are known to be more readily decomposed thermally than hydrocarbons, and thus would be expected to exhibit higher minimum ignition pressures.

Support for this thesis was obtained by limited thermogravimetric analysis studies. We found that the ANP 2969KH-1 binder lost 50 percent of its weight by being heated to 220°C, while the binders of ANB-3066, ANB-3105, and our model propellants required heating at the same rate to about 410°C for the comparable 50-percent weight loss.

Additional support for our identification of the relationship between binder type and minimum pressure for ignition comes from the results of some low pressure ignition studies done for another Institute program.<sup>11</sup> The variation in minimum ignition pressure was found to be small with wide compositional changes (such as content of aluminum, burning rate catalyst, and total solids), provided two basic ingredients are present--a binder of constant formulation and ammonium perchlorate. The nature of the oxidizer is, of course, also a factor of primary importance to the minimum ignition pressure.

2. Ignitability in the pressure-independent region. The general level of ignitability is the characteristic of ignition which is most variable among propellants. The test results show the tendency for the underoxidized systems to require more energy for ignition. Stoichiometry is undoubtedly a factor, such as the AP:CE<sub>2</sub> ratio, which eliminates consideration of the aluminum in the ignition reactions. After examining several possible interactions among composition and ignitability, it became obvious that burning rate, a ballistic parameter which is a net result of compositional variation, was most likely to correlate with level of ignitability.

Since the test data are expressed at different fluxes and in different manners for all the compositions studied, we decided to use surface temperature at ignition as a measure of ignitability; i.e., that propellant which has the lower  $T_s$  at ignition is the more readily ignitable and is ignited in less time. Thus, regardless of the validity or accuracy of the absolute value of the calculated surface temperature at ignition, it does provide a general measure of energy required for ignition.

In calculating the surface temperature at ignition for the several compositions studied, no account was taken of propellant absorptivity. Spectral reflectivity measurements of propellant surfaces at room temperature show that about 80 to 90 percent of the incident flux is likely to be absorbed at the surface. Since such measurements may not be valid under the conditions encountered during exposure to high thermal flux irradiation, we assumed that the absorptivities of all compositions were essentially the same and, for simplicity of calculation, equal to 1.0. Thus, calculated temperatures might be more realistic if they were reduced by about 10 to 15 percent.

Surface temperatures were calculated using the solution to the general heat conduction equation in the absence of chemical reaction. The propellant is regarded as an inert, perfectly absorbing, homogeneous, semi-infinite slab on which is incident a constant uniform flux,  $\phi$ . Evans et al.<sup>12</sup> have discussed some consequences of inhomogeneity and have demonstrated that the propellant specimen is effectively semi-infinite, with heat flow being one-dimensional, at least for the shorter times considered here. The expression used for calculating surface temperature is thus<sup>13</sup>

$$T_s - T_i = \frac{2\phi}{(k\rho)^{1/2}} \left( \frac{\tau}{\pi} \right)^{1/2} \quad (1)$$

where  $T_i$  = the initial surface temperature (assumed to be 24°C)

$T_s$  = surface temperature at time  $\tau$  (°C)

$\phi$  = radiant flux (cal/cm<sup>2</sup>-sec)

$(k\rho)^{\frac{1}{2}}$  = average "thermal responsivity" of the propellant.

Although thermal conduction (k), specific heat (c), and density ( $\rho$ ) may vary considerably among the various compositions studied, the thermal responsivity is reasonably constant. These values were measured in some cases, obtained from Aerojet-General Corporation or from other references, or were estimated, to arrive at the values of thermal responsivity shown in Table V.

TABLE V

THERMAL RESPONSIVITY OF COMPOSITIONS

Composition	$(k\rho)^{\frac{1}{2}}$
Pellet Nos. 3,4,5,6	0.026
PBAN-254,259,260,264	0.0245
PBAN-256	0.024
PBAN-257	0.023
PBAN-258	0.022
ANB-3066	0.0242
ANP-2639AF	0.0233
ANP-2969KH-1	0.0248
ANP-2677	0.024

To achieve a common basis for correlation with burning rates, we calculated ignition temperatures from data on the high-pressure line of -2.0 slope of the  $\log \tau$  -  $\log \phi$  plots, or, if that was not available, from the values of  $\tau$  and  $\phi$  from the  $\log \tau$  -  $\log P$  plots at high pressure, where  $\tau$  was independent of pressure. Pellet surface temperatures were calculated from high-pressure data. Table VI lists these values of calculated surface temperature at ignition.

TABLE VI  
CALCULATED VALUES OF SURFACE TEMPERATURE

Composition	T <sub>s</sub> (High Pressure), °C
Pellet No. 3 (PBAN-254)	353
Pellet No. 4 (PBAN-259)	426
Pellet No. 5 (PBAN-260)	537
Pellet No. 6 (PBAN-264)	423
PBAN-254	264
PBAN-259	328
PBAN-260	326
PBAN-264	332
PBAN-256	391
PBAN-257	439
PBAN-258	554
ANB-3066	352
ANB-2969KH-1	509
ANP-2639AF	466
ANP-2677	424

Although the absolute values of these calculated temperatures are of questionable validity, they are used in this sense as measures of relative ignitability. From these data, one can make the following observations:

1. The catalyst CuO2O2 tends to lower the ignition temperature and to reduce the energy required for ignition.
2. Increased oxidizer loading also lowers the surface temperature or conversely, fuel enrichment increases the surface temperature and the energy required for ignition.
3. Pellet surface temperatures are about 100°C higher than for the comparable propellant composition (with the exception of PBAN-260), indicating that the presence of a pyrolyzable organic fuel eases ignition.
4. The polybutadiene-type propellants generally appear to be more readily ignitable than the polyurethane types.

Figure 28 shows the excellent correlation between calculated surface temperature and burning rate. The ignitability, as measured by surface temperature, appears to be proportional to burning rate; i.e., the higher burning rate propellant has the lower ignition temperature and is more readily ignited. The operational propellants are in excellent agreement with this finding; a possible exception is ANB-3105 (with a considerably higher burning rate than that of ANB-3066), whose ignition temperature, although not calculable at this time, would be expected to lie near that of ANB-3066.

The model propellants containing CuO2O2 appear to lie on a line approximately parallel to that of the operational propellants, but at higher burning rates. From the comparisons of pellet and propellant ignition temperatures in Table VI, we might infer that the PBAN-260 test data are in error and that the surface temperature should be about 100°C higher, putting it on the correlation line. It may also be possible that the lightly catalyzed PBAN-260 does not fit the correlation, but rather lies between the catalyzed and uncatalyzed systems. The uncatalyzed model propellants are on yet another

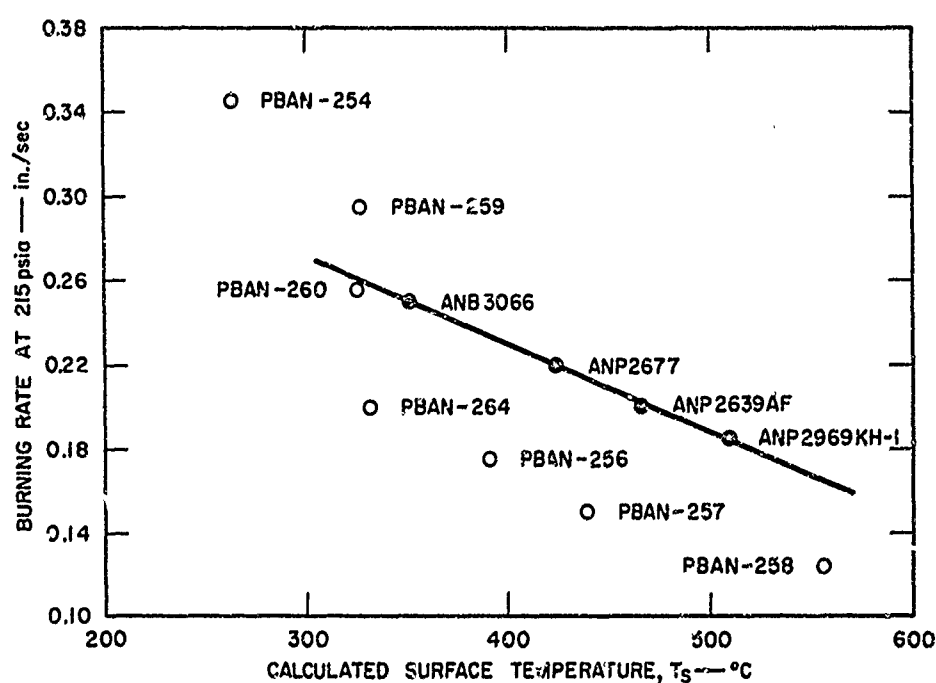


FIG. 28 CORRELATION BETWEEN BURNING RATE AND CALCULATED SURFACE TEMPERATURE AT IGNITION

approximately parallel line at lower levels of burning rate, with decreased ignition temperatures and higher burning rates accompanying higher solids loading.

Inferences concerning the influence of aluminum on ignition characteristics are not possible. The nonaluminized ANP-2677 data correlate well with those of the aluminized propellants. No other significant effect of aluminum is apparent. Thus we must conclude that aluminum acts as an inert material in the ignition processes and serves only to modify the thermal responsivity of the propellant.

### 3. Deviation from "constant ignition temperature" behavior.

As we have stated, in the absence of chemical reactions, a line of -2.0 slope on a  $\log \tau$  versus  $\log \phi$  plot represents a constant surface temperature. To avoid preempting the later discussion on ignition mechanisms, we now describe the deviation from the -2.0 slope line simply as deviation from constant ignition temperature behavior. Such deviation is also a measure of pressure dependence, in that as flux is increased, deviation from the constant slope line indicates the beginnings of pressure-dependent behavior.

Comparing the data for PBAN-254 and PBAN-264 (Figs. 10 and 15), we observe that the catalyst CuO202 appears to suppress the dependence on pressure in that the deviations from the -2.0 slope lines at both 14.7 and 215 psia are less extensive for PBAN-254. It is also interesting to note that the flux at which such deviation commences (at 14.7 psia) appears to be unaffected by catalyst content--i.e., it is about 28 cal/cm<sup>2</sup>-sec for both PBAN-254 and 264. Although the data for PBAN-257 (Fig. 18) are less extensive, it appears that increased binder content results in deviation from constant temperature behavior at lower flux levels and that the extent of the deviation is greater.

Thus, it appears that the same general conclusions can be reached as those obtained from examination of ignitability in the pressure-independent regime. Pressure dependency appears to be suppressed by the same factors that increase burning rate, namely, the presence

of burning rate catalyst and higher oxidizing solids loading. This generality appears to be valid, however, only in specific regions of pressure and flux; other patterns of behavior might well be observed under conditions not covered in this program.

### C. Mechanisms of Ignition

#### 1. General Discussion

Much discussion of the mechanisms of ignition has appeared in the literature and at technical meetings. To undertake a complete review would be both presumptuous and inconsistent with the scope of this program.

Two comprehensive reviews of ignition research and its results have been undertaken which cover the various works in detail. Although the reviewers have themselves been associated with particular mechanistic theories, they objectively compare the alternative approaches. Summerfield et al<sup>14</sup> describe the many research programs, present data, and evaluate results; Price et al<sup>15</sup> provide a detailed discussion of the phenomena associated with ignition and examine analytically the three major ignition theories, those which advocate the so-called condensed-phase, gas-phase, and heterogeneous ignition models.

Prior to undertaking this discussion, we shall take note of those specific points made by various investigators that are pertinent to the ignition models; recognizably cursory, such points of review are included here to establish a basis for the discussion to follow.

Condensed-phase model. Consideration of the condensed-phase model originated from bulk thermal explosion theory and was first discussed by Frazer and Hicks.<sup>16,17</sup> They derived a model which defined surface temperature on ignition as being calculable from a transient heating analysis which included a chemical heating term from condensed-phase, exothermic reaction. Altman and Grant<sup>18</sup> showed that at long times and low fluxes the chemical heating term could be neglected, and that ignition was characterized by a constant surface temperature.



Baer and Ryan<sup>9</sup> reported that under conditions of low heat flux, pressure had no effect on the ignition process. As discussed earlier, the work in both Refs. 9 and 18 involved maintaining external stimulus through the ignition phase. Price et al<sup>19</sup> extend the condensed-phase ignition theory by accounting for such effects as reactant depletion and by suggesting that deviations of experimental results from what might be predicted by the constant surface temperature concept indicate that the ignition temperature in fact increases at high heating rates.

Gas-Phase Model. Since pressure and oxygen concentration in the gaseous environment were found to be important factors in composite propellant ignition, a model was proposed in which the major exothermic processes leading to "runaway" conditions were governed by gas phase kinetics. Summerfield et al<sup>14</sup> describe the extensive studies which provide pertinent evidence for this theory. Anderson and Beyer<sup>6</sup> and Price<sup>15</sup> state that the theory is not applicable because the analysis did not account for both fuel and oxidizer gases being generated by propellant decomposition. Price et al<sup>20</sup> suggest that, at high heating rates, a gas-phase ignition regime might indeed exist in which ignition is dependent upon generation of gaseous reactants and the flow of energy from the gas phase back to the solid surface. Such processes need not require large quantities of gaseous reactants but may occur upon first gas formation, as indicated by the results of Evans et al<sup>12</sup>

Heterogeneous Model. Based on results of studies of hypergolic ignition (heterogeneous reaction between an external reactive oxidizer and a solid fuel), Anderson et al<sup>6,21</sup> propose that the ignition process is governed by the kinetics of the heterogeneous reaction between ammonium perchlorate decomposition products and the solid fuel. They further propose that this reaction takes place at the oxidizer-fuel interface within the surface layer of the propellant. Evidence for validity of the theory is cited as the relationship  $\tau \propto P^{-2.15}$  at low pressures. Price<sup>15</sup> reviews all the assumptions made

and evidence quoted and suggests that clear-cut proof of the model has not yet been provided. Our program has shown that the relationship at low pressures is not  $\tau \propto P^{-2.15}$ , but that  $\tau$  instead approaches an asymptote of infinite slope at the minimum ignition pressure.

## 2. Definition of Time to Ignition

The total ignition process can be divided into time intervals representing a coarse division of associated phenomena. Thus, the division of ignition has been represented as

$$\tau = \tau_1 + \tau_2 + \tau_3 \quad (2)$$

where  $\tau$  = total time to ignition

$\tau_1$  = time of surface temperature increase by external stimulus not originating from the propellant itself

$\tau_2$  = time of heat addition to the solid by exothermic chemical reaction, i.e., solid phase decomposition, feedback from gas-phase reaction, heterogeneous reaction within the surface layer

$\tau_3$  = time of transition to steady-state combustion.

The experimental approach used in this program, which utilized radiant energy as the external stimulus, yields data based on a threshold ignition time obtained by go/no-go tests. Ignition time is defined as that time of exposure to a radiant flux which is necessary for steady-state combustion to be achieved at the time of, or at some delayed time after, cessation of the external stimulus. This time required for establishment of the steady-state flame, after cessation of external stimulus, might be termed the delay time, equivalent to  $\tau_3$ . The exposure time determined in this research is  $\tau_1$ . It is generally recognized that in such cases as ignition at high pressure,  $\tau_2$  and  $\tau_3$  are small compared to  $\tau_1$  and, from an experimental viewpoint, can be neglected. However, at long exposure times (i.e., at low fluxes and/or pressures),  $\tau_2$  may become significant; and under some conditions, measured values of  $\tau_3$  have been large compared to  $\tau_1$ .<sup>1</sup>

We note that by definition  $\tau_1$ ,  $\tau_2$ , and  $\tau_3$  need not be considered as chronologically ordered time periods. Retaining  $\tau_3$  as the post-exposure delay time in our experimental approach, Eq. (2) would be more correctly written as

$$\tau = \tau_1 + \tau_3 \quad (3)$$

where time of exothermic heat addition,  $\tau_2$ , is now composed of some unknown portion of  $\tau_1$  and all of  $\tau_3$ . Full definition of the time,  $\tau_2$ , is of course the ultimate objective, if understanding of the ignition mechanisms is to be achieved.

The experiments which utilize sustained external stimulus through the ignition process and yield ignition times identified by the appearance of first light do not provide a terminus value of  $\tau_2$  because sustained combustion is not assured should the external stimulus be removed after the appearance of first light. Anderson and Beyer<sup>3</sup> showed that light can be emitted and detected during a nonignition exposure. Friedman and Levy<sup>22</sup> measured burning rates of pressed ammonium perchlorate strands at pressures far below minimum combustion pressures by maintaining an external stimulus during the experiment. In our studies, we exposed pellets of pressed ammonium perchlorate/carbon compositions to radiant energy; although sustained combustion was not attainable, extensive flame development was apparent while the energy was being applied.

With our experimental approach,  $\tau_2$  is not defined either, but a mechanistically important portion of it is separable. The delay time,  $\tau_3$ , is that portion of  $\tau_2$  which persists after cessation of external stimulus. Past work<sup>1</sup> has shown that at a relatively high flux  $\tau_3$  is effectively zero at low pressures, increases to a maximum in a moderate pressure range, then decreases to zero as pressure continues to increase. Extension of these observations would undoubtedly be useful in at least a qualitative assessment of  $\tau_2$  and the relative roles of the various potential exothermic reactions.

For example, at low pressures, heating from the gas phase might be discounted and external stimulus might be required for the total time  $\tau$  to overcome endothermic processes. As pressure is increased, gas-phase kinetics may become more important, leading to measureable values of  $\tau_g$ . Finally, at high pressure, gas-phase reaction rates might increase to the extent that  $\tau_g$  again becomes negligible. Similar reasoning can be applied to a heterogeneous ignition model, and even to a condensed-phase decomposition model; in the latter case, pressure could act on gaseous products to either increase or decrease rate of decomposition, or pressure could have no influence at all. A fruitful avenue for future investigation appears to be the inclusion of  $\tau_g$  measurement under all conditions in the full characterization of ignition behavior.

### 3. Concept of Constant Ignition Temperature

The constant surface temperature concept appears to be valid under those conditions where  $\log \tau - \log \phi$  data fall on a line of -2.0 slope. Such appears to be the case at high pressures and at low heating rates. However, as heating rate, or flux, is increased, pressure dependence is demonstrated by the departure of the data from the "constant temperature" line. Increasing pressure at a constant level of high flux serves to reduce ignition times until they again reach the constant temperature line.

It is incorrect to assume that the surface temperature is calculable in the pressure-dependent regime by the solution to the transient heating equation; a calculated surface temperature of 720°C, for example, for PLN-264 at 14.7 psia and 100 cal/cm<sup>2</sup>-sec is hardly conceivable. One might equally assume that the ignition temperature is effectively constant under all conditions, and that endothermic heat sinks act to increase the required exposure time until the characteristic surface temperature is reached. Dissociation of ammonium perchlorate and binder pyrolysis are such endothermic processes, and their contribution to the heating requirements must be taken into account.

More detailed examination of this assumption of constant temperature at ignition results in some anomalies, which in turn leaves the more realistic postulate that  $T_g$  is probably not constant but is likely to be a rising function with flux in the pressure-dependent regime. Further, in considering the applicability of a characteristic ignition temperature, the results of our work which indicate that such a characteristic temperature may also be pressure-dependent, must also be taken into account.

#### 4. Ablation

Contrary to the general belief, deviation from  $\log \tau - \log \phi$  line of -2.0 slope is not necessarily accompanied by ablation. Anderson and Beyer,<sup>6</sup> in Fig. 4-1 of their report, show the beginning of ablation at the -2.0 slope line and its continuation until ignition is achieved. Studies of the double bass composition JPN, in which weight loss was measured, appeared to verify this assumption.<sup>20</sup> However, in our program, specimens of PBAN-260, 264, and 258 were weighed before and after exposure for times shorter than required for ignition. Table VII shows the results of these tests.

From these data, it is apparent that except for the underoxidized composition PBAN-258, ablation not only does not commence at the line of -2.0 slope, but may not even be extensive near ignition. Fumes did appear at much shorter times than those at which weight loss became measurable. Support is thus provided for the suggestion by Bastress<sup>7</sup> that pyrolysis of surface material yields gaseous hydrogen and a char residue. The endothermic processes in composite propellants are either of small consequence or are almost entirely condensed-phase processes.

TABLE VII

## WEIGHT LOSS DURING NONIGNITION EXPOSURES

Composition	Pressure, psia	Flux cal/cm <sup>2</sup> -sec	$\tau$ , msec	Weight Loss, %	Remarks
PBAN-260	14.7	65	27.5	---	Ignition
	14.7	65	27.5	0.1	
	14.7	65	26.5	0.1	
	14.7	65	24	0	
	215	65	10	---	Ignition
PBAN-26	7.4	65	65	---	Ignition
	7.4	65	65	1.8	
	7.4	65	62	1.0	
	7.4	65	50	0.7	
	14.7	65	38	---	Ignition
	215	65	13	---	Ignition
	7.4	12	410	---	Ignition
	7.4	12	392	0.2	
	7.4	12	330	0.1	
PBAN-258	7.4	65	180	---	Ignition
	7.4	65	165	2.3	
	7.4	65	137	1.8	
	7.4	65	118	1.3	
	7.4	65	63	0.9	
	7.4	65	38	0.4	
	7.4	65	20	0.1	
	7.4	12	390	---	Ignition
	7.4	12	375	1.0	
	7.4	12	330	0.5	
	7.4	12	316	0.1	

## 5. Ignition Models

In examining the various ignition models, we observe that the question of the chemistry involved in achieving steady-state combustion remains unresolved. Arguments in favor of condensed-phase, gas-phase, or heterogeneous exothermic reaction can be put forth with conviction under all conditions. It becomes readily apparent that more information is required.

The true nature of the propellant surface, being nonhomogeneous, enables consideration of different temperatures of binder and oxidizer. Hence, gas-phase reactions at calculated temperatures below those required for binder pyrolysis are conceivable; deflagration of ammonium perchlorate before the occurrence of other exothermic reactions is possible; and heterogeneous reactions are readily visualized.

Only in the case of solid-phase, thermal decomposition of ammonium perchlorate is the requirement for oxidizing gases eliminated. Dissociation pressure measurements of ammonium perchlorate<sup>23</sup> indicate that at about 300°C--a reasonable calculated surface temperature for any of our propellants--the dissociation pressure was only about 0.4 mm Hg. It was also observed that dissociation and thermal decomposition could occur simultaneously. Further, the temperature of the ammonium perchlorate is likely to be below that calculated for the homogeneous surface. However, since nonequilibrium conditions most likely prevail during ignition, a reasonable concentration of  $\text{HClO}_4$  might be expected if  $\text{NH}_3$  is removed from the reaction zone rapidly enough. Evans et al<sup>22</sup> show that the solid-phase decomposition exotherm is an unlikely contributor from kinetic considerations. On the other hand, decomposition kinetics under high heating rates and nonequilibrium conditions might be such that condensed-phase reactions become possible in the Evans temperature-time frame.

The purely chemical approach has thus far not succeeded in clarifying the controlling mechanisms of ignition. Another approach is proposed by von Elbe,<sup>24</sup> and in the light of the results of this program, appears to warrant detailed examination. His model for steady-state combustion

includes a characteristic surface temperature,  $T_g$ , at which gasification of the propellant occurs. Simplified relationships among heat flow to the surface, burning rate,  $T_g$ , and propellant thermal properties are presented. He proposes that the time,  $\tau$ , at a specific value of externally applied heat flux is required for the surface temperature to reach  $T_g$  during ignition. At this point, we question the suggestion that surface temperatures are equal under steady-state burning conditions and at ignition, but further examination of the model need not be interrupted.

If the external stimulus is applied at a rate of less than or equal to the steady-state burning feedback flux, sufficient energy is available within the subsurface layers for ignition to succeed. Expressed in another manner, the temperature profile is as flat as or flatter than that during steady-state combustion. If the applied flux is greater than the steady-state flux, the profile will be steeper than that at steady-state, and the temperature  $T_g$  will fall. von Elbe uses the term "preheat" to define the integral of the temperature profile, or the quantity of energy that has been transported into the solid in the time  $\tau$ .

von Elbe further suggests that, at high fluxes, after the "flash" temperature,  $T_g$ , has been reached, the surface ablates so that the preheat cannot increase to that required for successful ignition. However, he suggests that there is some mechanism which adjusts the flux, thereby enabling the profile to flatten and the preheat to increase. We believe a more likely explanation than flux adjustment is simply that time is required for heat to flow into the solid to establish the required temperature profile. The surface temperature may either exceed the characteristic surface temperature or it may remain constant, while the integral of the temperature profile increases to the required level. Temperature-limiting endothermic reactions during this period may include binder pyrolysis and ammonium perchlorate dissociation, as well as gasification or ablative processes.



need not occur to any great extent. In our brief studies of specimen weight loss during exposure, it is obvious that only minor ablation occurs and most of that occurs very near the actual ignition point.

In terms of our results, this hypothesis suggests that ignition occurs along the line of -2.0 slope on a plot of  $\log \tau - \log \phi$  at values of  $\phi$  below that equal to the steady-state feedback flux. At fluxes higher than the steady-state  $\phi$ , the ignition time deviates from the -2.0 slope line to longer times to enable the equivalent of the steady-state preheat to be established. von Elbe's equations are

$$q = \phi \tau \text{ and } q_0 = \phi_0 \tau, \text{ cal/cm}^2 \quad (4)$$

$$\phi_0 = r_0 c \rho (T_s - T_i), \text{ cal/cm}^2\text{-sec} \quad (5)$$

where  $q$  = preheat, or integral of the temperature profile

$q_0$  = preheat under steady-state burning conditions

$\phi_0$  = steady-state feedback flux

$r_0$  = steady-state burning rate

$c$  = specific heat of the propellant

$\rho$  = density of the propellant.

Using Eqs. (4) and (5), we have calculated values of  $\phi_0$  and  $q_0$  for some of our test compositions; these are compared in Table VIII with the experimental results obtained from Figs. 10, 13, 15, 18, and 22. Agreement between calculated values and experimental values is reasonably good. Exceptions at 215 psia illustrate possible errors in absolute values of measured flux, as discussed earlier; disagreement at 14.7 psia may illustrate the invalidity of the model at low pressure. These results indicate that, at 215 psia, the preheat required for ignition of the uncatalyzed model systems (PBAN-264 and 257) is much less than that for those compositions having catalyst (PBAN-254 and 260); at 14.7 psia catalyst content does not appear

TABLE VIII

## STEADY-STATE FLUX AND PREHEAT FROM VON ELBE'S MODEL

Composition	Pressure, psia	Calculated		Experimental	
		$q_0$	$q_0$	$q_0$	$q_0$
PBAN-254	215	48	0.53	50	0.55
	14.7	13	0.8	28	1.7
PBAN-260	215	45	0.5	60	0.66
	14.7	10	1.2	18	2.2
PBAN-264	215	36	0.1	36, 56	0.1, 0.16
	14.7	11	1.0	28	2.5
PBAN-257	215	35	0.09	40	0.1
ANB-3066	215	46	2.5	30	1.4
	35	44	2.4	48	2.6

to influence preheat requirements significantly. The propellant ANB-3066 appears to require considerably more preheat than the catalyzed model compositions, presumably due to the aluminum present.

Still in question, however, is identification of the process or combination of processes operative during the time the temperature profile is adjusting at flux levels higher than  $q_0$ . There is no reason to believe at this time that such processes are too dissimilar from those which lead to a fully developed flame at low fluxes where test data conform to the line of -2.0 slope. Having reached a characteristic surface temperature in the latter case, chemical reaction rates are such that the additional time required in the "runaway" reaction is likely to be small in comparison to the thermal conduction time. Similarly, at flux levels above  $q_0$ , these same "runaway" reactions are likely to occur, but for them to be sustained, the condition of sufficient preheat must also be satisfied.

In this discussion it should be noted that the final exothermic "runaway" process could be controlled by gas-phase, condensed-phase, or heterogeneous reaction kinetics, or by any combination of them. The model describes ignition characteristics in terms of thermal conduction and steady-state burning rate only; the "runaway" reaction is merely the short-time, terminal phase which requires specific thermal conditions for successful initiation.

To illustrate the feasibility of the model proposed by von Elbe, we determined the required times, using a computer to obtain the numerical solutions to the transient heat conduction equation. Required input data were taken from the results of tests of PBAN-254 and the thermal properties of that composition were used. Integrals of the temperature profile and the time required for a surface temperature rise of  $240^{\circ}\text{C}$  were computed for  $\phi_0$  equal to 30 and 50 cal/cm<sup>2</sup>-sec, representing the points of deviation from the line of -2.0 slope at 14.7 and 215 psia, respectively. Additional times required to achieve the integral values of preheat at  $\phi_0$  for fluxes greater than  $\phi_0$  were then computed under two assumptions: (1) that  $T_s - T_i$  remained constant at  $240^{\circ}\text{C}$  throughout the process; and (2) that  $T_s$  increased according to an arbitrarily selected function of  $\phi$ . Input values used for individual point computations are shown in Table IX.

It can be seen from the computation results shown in Fig. 29 that the data representing the pressure-sensitive regime are indeed similar to experimentally determined values. When surface temperature is assumed to be constant, as in curves A and C, the shape of the curve is similar to that for PBAN-260 (Fig. 13). Curves B, D, and E are similar to the more general case, such as PBAN-254 (Fig. 10). It should be noted that the straight line reflects the linear relationships arbitrarily selected between  $T_s$  and  $\phi$ .

Although the von Elbe model can thus be used to predict ignition data which are very similar to those measured experimentally, the possible contributions by chemical reactions are not eliminated.

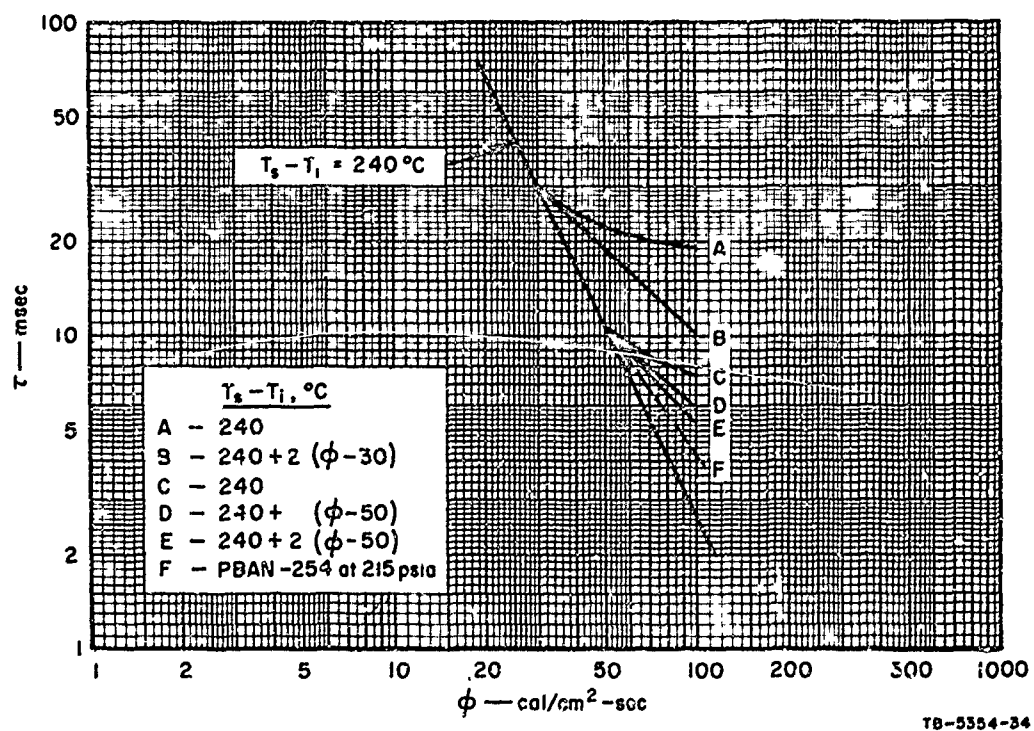


FIG. 29 DEPENDENCE OF EXPOSURE TIME ON FLUX: CALCULATED TIMES ACCORDING TO VON ELBE'S MODEL.

TABLE IX  
INPUT DATA FOR CONDUCTION TIME COMPUTATIONS

$\phi_0$ , cal/cm <sup>2</sup> -sec	$\phi$ , cal/cm <sup>2</sup> -sec						
	40	50	60	70	80	90	100
30	240	240	240	240	240	240	240
30	260	280	300	320	340	360	380
50	---	---	240	240	240	240	240
50	---	---	250	260	270	280	290
50	---	---	260	280	300	320	340

Note: Tabulated values are  $T_s - T_1$ , in °C.

Exothermic reactions may still add heat to reduce the time required to establish the necessary preheat. Since Fig. 29 was based on PBAN-254, the experimental curve F appears to be a straight line, but is of greater slope than curve E. This indicates either that added heat from chemical reaction results in shorter than calculated times, or that  $T_s$  increases to larger values than assumed for curve E.

Figure 30 is a plot of  $\log \phi\tau$  (the preheat, or ignition energy) versus  $\log \phi$  for the test data of PBAN-260. The constant  $T_s$  line (in the absence of chemical reaction) on this type of plot has a slope of -1.0 (curve A). Ignition energies at 14.7 psia lie along curves A and B; ignition energies at 215 psia lie along curves A and D. In terms of von Elbe's thesis, the preheat  $\phi\tau$  deviates from the line of -1.0 slope to allow time for establishment of the required integral of the temperature profile at  $\phi_0$ . [It is of interest to note that the additional energy required, plotted as  $\log \phi\tau$  versus  $\log \phi$ , and shown as curves C and E (B minus A, and D minus A, respectively) appears to approach a slope of +1.0 as  $\phi$  gets large. Lines of slope equal to +1.0 on such a plot represent constant times.]

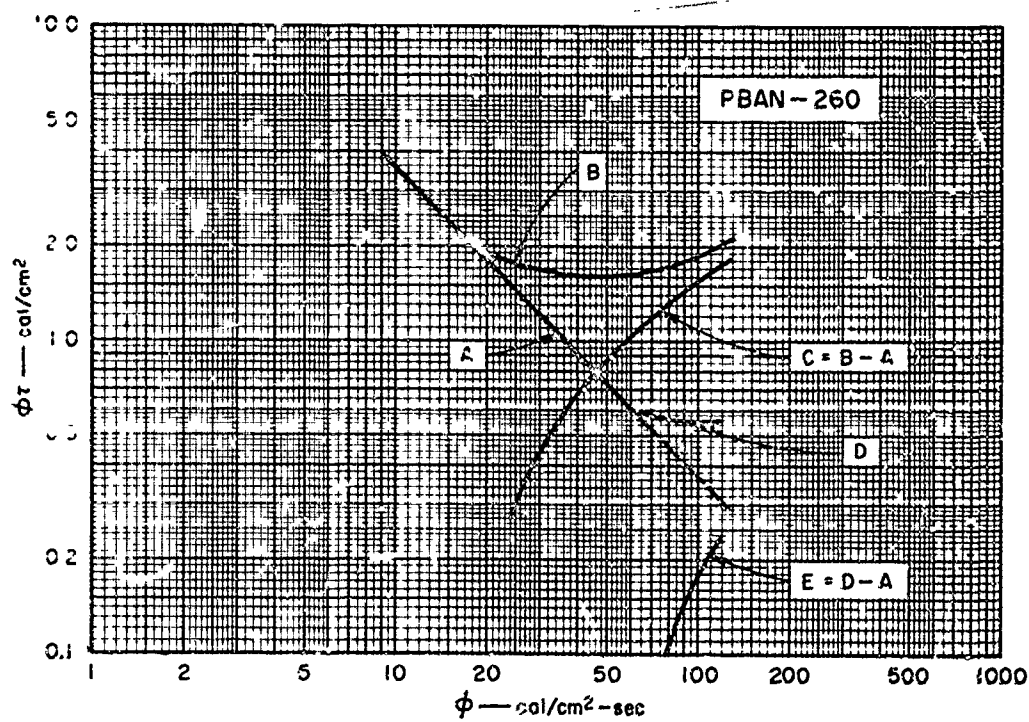


FIG. 30 TYPICAL RELATIONSHIP BETWEEN IGNITION ENERGY AND INCIDENT FLUX

Computed data shown in Fig. 29 are replotted as  $\log \varphi \tau$  versus  $\log \varphi$  in Fig. 31. Again, as in Fig. 29, we observe that the computed data are quite similar to experimental results. Perhaps the most important difference is the lack of curvature shown in curve B of Fig. 30. Curve B can probably be simulated by computation according to von Elbe's model, if  $T_s$  were first a rapidly increasing function of flux and then held constant and independent of  $\varphi$ .

The von Elbe model does not provide for energy being supplied by heterogeneous or condensed-phase chemical reaction, and perhaps such exothermic energy is small when the temperature profile in the solid is very steep. However, as the preheat increases, the contribution of energy from exothermic chemical reactions could become substantial. Thus, the appropriate combined consideration of energy of endothermic and exothermic chemical reactions and the time required for conduction of heat from the surface is a more realistic model. Accordingly, computations which include the chemical contributions are more likely to yield the characteristics determined experimentally.

Thus, it appears that the model proposed by von Elbe provides a reasonable qualitative, if not wholly quantitative, explanation for the ignition behavior of propellants. The prime contribution of his model is to explain observed "pressure-dependent" behavior in terms of burning rates and temperature profiles in the solid material. Not yet accounted for, however, are the contributions from chemical reaction. This model provides what appears to be a realistic approach toward understanding the mechanism of ignition by coupling it to steady-state combustion.

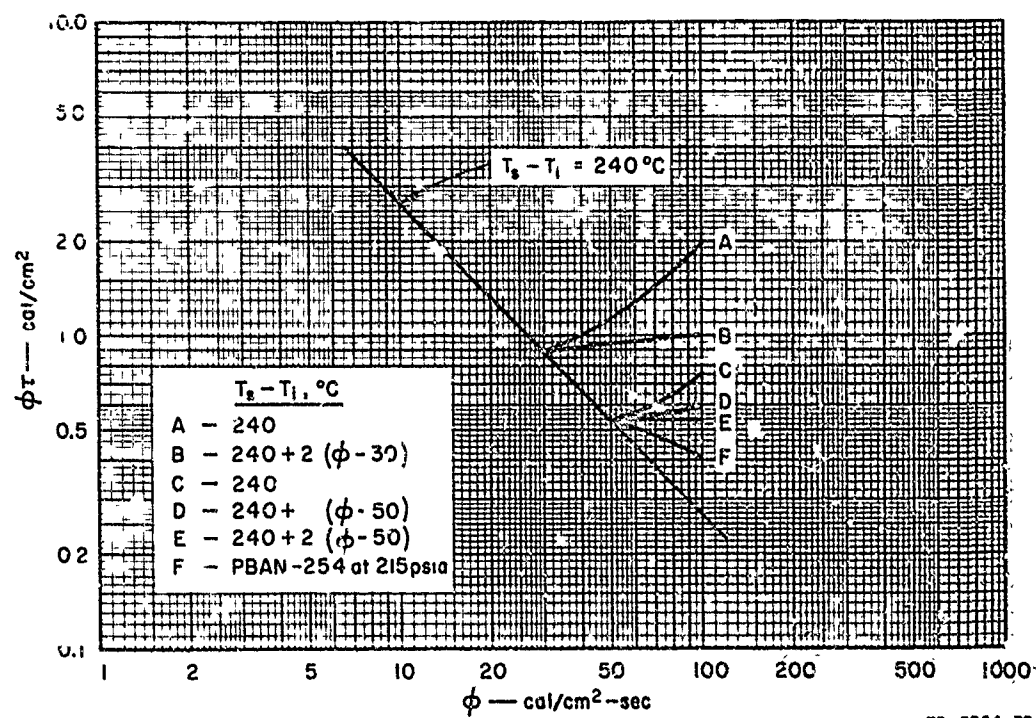


FIG. 31 RELATIONSHIP BETWEEN IGNITION ENERGY AND INCIDENT FLUX:  
DATA CALCULATED ACCORDING TO VON ELBE'S MODEL



## V SUMMARY AND CONCLUSIONS

The ignition characteristics of five operational propellants and seven model systems of varying composition were investigated by the use of high flux radiant energy as the ignition stimulus. The Stanford Research Institute arc image ignition furnace was improved to provide higher flux capability, greater arc stability, and greater ease of operation.

Examination of experimental results yielded the following typical ignition characteristics:

1. Pressure-independent behavior (high pressures) is characterized by test data which lie on a slope equal to -2.0 on plots of log exposure time versus log flux.
2. In the regions of apparent pressure-independence, ignition (assuming no chemical reaction) is characterized by a constant surface temperature.
3. The logarithmic relationship between exposure time and pressure is typified by asymptotes of infinite slope at the minimum pressure for ignition, and of zero slope at high pressures.
4. The minimum pressure for ignition appears to be independent of flux.
5. The influence of pressure on ignition at pressures above the minimum is highly dependent on flux.

Surface temperatures at ignition were calculated from experimentally determined values of exposure time and flux, and were used as measures of ignitability in the pressure-independent regime. An excellent correlation was established between burning rate and surface temperature at ignition; higher burning rates are related to lower ignition temperatures. The burning rate catalyst Cu O2O2 lowers the ignition temperature, as does increased oxidizer content. The presence of a pyrolyzable organic fuel eases ignition, as indicated by comparison of propellant test results with those of pressed pellets containing no binder. Aluminum does not appear to influence ignitability, except

as it modifies the thermal properties of the propellant. Pressure dependency is suppressed by the same factors which increase burning rate. The minimum pressure for ignition of ammonium perchlorate propellants appears to be primarily related to the nature of the binder.

Various ignition theories were examined in the light of the information developed on this and other programs. The heterogeneous theory of ignition is not supported by our data particularly since the log time versus log pressure data do not approach the predicted slope of -2.15 at low pressures. Pressure-dependency has been cited as an argument in favor of both the heterogeneous and gas-phase ignition models; however, if pressure is considered to influence ignition behavior because of its effect on the rate of burning, condensed-phase decomposition reactions cannot be excluded. The von Elbe ignition model, which relates ignition characteristics to steady-state combustion and propellant thermal properties, was examined and found to provide a promising initial framework for explaining observed behavior. It was concluded that the case for any of the chemical reaction mechanisms controlling ignition has not been proved, and that, although chemistry is certainly involved in the runaway reactions and in processes which might limit surface temperature, chemical reaction kinetics may not be of primary importance to ignition times. It appears likely that the total time-to-ignition is composed primarily of the thermal induction period controlled by heat transfer processes, the delay time, which is controlled by chemical reaction kinetics, is vanishingly small under many conditions.

#### REFERENCES

1. Beyer, R. B. and N. Fishman, "Solid Propellant Ignition Studies with High Flux Radiant Energy as a Thermal Source," Solid Propellant Rocket Research, Progress in Astronautics and Rocketry, Vol. I, Academic Press, 1960, pp. 673-692.
2. Bureau of Naval Weapons Contract No. N0w 65-0198-d, "Ignition of Solid Rocket Propellant Surfaces," SRI Project No. GHU-5277, D. B. Moore and M. W. Evans.
3. Beyer, R. B., L. McCulley, and M. W. Evans, "Measurement of Energy Flux Density Distribution in the Focus of an Arc Image Furnace," Applied Optics Vol. 3, No. 1, January 1965, pp 131-135.
4. Hightower, J. D., NOTS Memorandum, "Comparative Calibration of Calorimeters," 20 April 1965.
5. Gardon, R., "An Instrument for the Direct Measurement of Intense Thermal Radiation," Rev. Sci. Instr. 24, 366-370 (1953).
6. United Technology Center Final Report on Contract No. AF 04(611)-9701 "Ignition of Solid Propellant Motors under Vacuum," 8 April 1965.
7. Arthur D. Little, Inc. Technical Documentary Report No. RPL-TDR-64-65 on Contract No. AF 04(611)-9065, "Solid Propellant Ignition Studies," 30 October 1964.
8. Proceedings of the Third Meeting of the JANAF Ignitability Panel, Applied Physics Laboratory, Silver Spring, Md., June 19, 1959.
9. Baer, A. D., and N. W. Ryan, "Ignition of Composite Propellants by Low Radiant Fluxes," AIAA Preprint No. 64-119, Solid Propellant Rocket Conference, Jan. 29-31, 1964.
10. Hightower, J. D., NOTS letter to Participants, Interlaboratory Solid Propellant Ignition Exchange Program, 15 October 1964.
11. NASA Contract No. NAS 7-389, "Propellant Combustion Phenomena during Rapid Depressurization," SRI Project no. FRU-5577. L. A. Dickinson and E. L. Capener.
12. Evans, M. W., R. B. Beyer, and L. McCulley, "Initiation of Deflagration Waves at Surfaces of Ammonium Perchlorate - Copper Chromite-Carbon Pellets," J. Chem. Phys. 40, 2431-2438 (1964).
13. Carslaw, H. S. and J. C. Jaeger, "Conduction of Heat in Solids," Second Edition, Oxford University Press, 1959.

14. Summerfield, M., R. Shinnar, C. E. Hermance, and J. Wenograd, "A Critical Review of Recent Research on the Mechanism of Ignition of Solid Rocket Propellants," Aeronautical Engineering Laboratory Report 661, Princeton University, 26 August, 1963.
15. Price, E. W., H. H. Bradley, Jr., G. L. Dehority, and M. M. Ibiricu, "Theories of Ignition of Solid Propellants - A Review," NavWeps Report No. 8682 (NOTS TP 3743), to be presented at the 2nd ICRPG Combustion Conference, 1-5 November, 1965.
16. Frazer, J. H. and B. L. Hicks, "Thermal Theory of Ignition of Solid Propellants," J. Phys. Coll. Chem. 54, No. 6, pp. 872-6 (1950).
17. Hicks, B. L. "Theory of Ignition Considered as a Thermal Reaction," J. Chem. Phys. 22, No. 3, 414-29 (1954).
18. Altman, D. and A. F. Grant, Jr., "Thermal Theory of Solid Propellant Ignition by Hot Wires," Fourth Symposium (International) on Combustion, pp. 158-161, 1953.
19. Price, E. W., H. H. Bradley, Jr., J. D. Hightower, and R. O. Fleming, Jr., "Ignition of Solid Propellants," AIAA Preprint No. 64-120, Solid Propellant Rocket Conference, Jan. 29-31, 1964.
20. Price, E. W., H. H. Bradley, Jr., and R. Fleming, "Ignition of Solid Propellants," presented at Western States Section of the Combustion Institute, San Diego, California, 29-30 April, 1963.
21. Anderson, R., R. S. Brown, and L. J. Shannon, "Ignition Theory of Solid Propellants," AIAA Preprint No. 64-156, Solid Propellant Rocket Conference, Jan. 29-31, 1964.
22. Friedman, R., and J. B. Levy, "Further Studies of Pure Ammonium Perchlorate Deflagration," Eighth Symposium (International) on Combustion, pp. 663-672, 1960.
23. Inami, S. H., W. A. Rosser, and H. Wise, "Dissociation Pressure of Ammonium Perchlorate," J. Phys. Chem. 67, 1077(1963).
24. von Elbe, G., "Theory of Solid Propellant Ignition and Response to Pressure Transients," Bulletin of the 18th Interagency Solid Propulsion Meeting, CPIA No. 18, Vol. III, pp. 95-127, June, 1963.

UNCLASSIFIED

Security Classification

DOCUMENT CONTROL DATA - R&D

(Security classification of title, body of abstract and indexing annotation must be entered when the overall report is classified)

1. ORIGINATING ACTIVITY (Corporate author)		2a. REPORT SECURITY CLASSIFICATION	
STANFORD RESEARCH INSTITUTE		Unclassified	
		2b. GROUP	
3. REPORT TITLE			
SOLID PROPELLANT IGNITION STUDIES			
4. DESCRIPTIVE NOTES (Type of report and inclusive dates)			
Final Report -- February 1 to September 1, 1965			
5. AUTHOR(S) (Last name, first name, initial)			
Fishman, Norman (n)			
6. REPORT DATE		7a. TOTAL NO. OF PAGES	7b. NO. OF REFS
November 5, 1965		83	24
8a. CONTRACT OR GRANT NO.		9a. ORIGINATOR'S REPORT NUMBER(S)	
AF 04(611)-10534			
b. PROJECT NO.			
3059			
c.		9b. OTHER REPORT NO(S) (Any other numbers that may be assigned this report)	
Program Structure No. 750G		AFRPL-TR-65-213	
d.			
10. AVAILABILITY/LIMITATION NOTICES			
Availability notice (1). Release to OTS not authorized			
11. SUPPLEMENTARY NOTES		12. SPONSORING MILITARY ACTIVITY	
		Air Force Rocket Propulsion Laboratory Research and Technology Division Air Force Systems Command, Edwards, Calif.	
13. ABSTRACT			
<p>The ignition characteristics of five operational propellants and seven model systems of varying composition were investigated by the use of high flux radiant energy as the ignition stimulus. Our study has provided considerable information which relates ignition characteristics to compositional factors. Findings of particular importance are:</p> <ol style="list-style-type: none"><li>1. For the types of propellants studied, ignitability is directly related to burning rate; within each system, those factors which increase burning rate also ease ignition.</li><li>2. Minimum pressure for ignition of ammonium perchlorate propellants appears to be primarily related to the nature of the binder.</li></ol> <p>We examined the various theories of ignition and found that no model yet suggested has been adequately proved. In applying von Elbe's model, we showed that the observed pressure-dependency of ignition could be related to steady-state combustion characteristics of the propellant, and that thermal conduction into the sub-surface material may contribute substantially to ignition time. We believe that we have placed the suggested mechanisms in proper perspective, so that identification can be made of the additional information required for fuller understanding of the important chemical processes.</p>			

DD FORM 1473  
1 JAN 64

Unclassified

Security Classification

UNCLASSIFIED

## Security Classification

14. KEY WORDS	LINK A		LINK B		LINK C	
	ROLE	WT	ROLE	WT	ROLE	WT
SOLID PROPELLANT IGNITION						
IGNITION MECHANISMS						
THEORIES OF IGNITION						
ARC IMAGE IGNITION FURNACE						

## INSTRUCTIONS

1. **ORIGINATING ACTIVITY.** Enter the name and address of the contractor, subcontractor, grantee, Department of Defense activity or other organization (*corporate author*) issuing the report.

2a. **REPORT SECURITY CLASSIFICATION:** Enter the overall security classification of the report. Indicate whether "Restricted Data" is included. Marking is to be in accordance with appropriate security regulations.

2b. **GROUP:** Automatic downgrading is specified in DoD Directive 5200.10 and Armed Forces Industrial Manual. Enter the group number. Also, when applicable, show that optional markings have been used for Group 3 and Group 4 as authorized.

3. **REPORT TITLE:** Enter the complete report title in all capital letters. Titles in all cases should be unclassified. If a meaningful title cannot be selected without classification, show title classification in all capitals in parenthesis immediately following the title.

4. **DESCRIPTIVE NOTES:** If appropriate, enter the type of report, e.g., interim, progress, summary, annual, or final. Give the inclusive dates when a specific reporting period is covered.

5. **AUTHOR(S):** Enter the name(s) of author(s) as shown on or in the report. Enter last name, first name, middle initial. If military, show rank and branch of service. The name of the principal author is an absolute minimum requirement.

6. **REPORT DATE:** Enter the date of the report as day, month, year, or month, year. If more than one date appears on the report, use date of publication.

7a. **TOTAL NUMBER OF PAGES:** The total page count should follow normal pagination procedures, i.e., enter the number of pages containing information.

7b. **NUMBER OF REFERENCES:** Enter the total number of references cited in the report.

8a. **CONTRACT OR GRANT NUMBER:** If appropriate, enter the applicable number of the contract or grant under which the report was written.

8b, 8c, & 8d. **PROJECT NUMBER:** Enter the appropriate military department identification, such as project number, subproject number, system numbers, task number, etc.

9a. **ORIGINATOR'S REPORT NUMBER(S):** Enter the official report number by which the document will be identified and controlled by the originating activity. This number must be unique to this report.

9b. **OTHER REPORT NUMBER(S):** If the report has been assigned any other report numbers (either by the originator or by the sponsor), also enter this number(s).

10. **AVAILABILITY/LIMITATION NOTICES:** Enter any limitations on further dissemination of the report, other than those

imposed by security classification, using standard statements such as:

- (1) "Qualified requesters may obtain copies of this report from DDC."
- (2) "Foreign announcement and dissemination of this report by DDC is not authorized."
- (3) "U. S. Government agencies may obtain copies of this report directly from DDC. Other qualified DDC users shall request through \_\_\_\_\_."
- (4) "U. S. military agencies may obtain copies of this report directly from DDC. Other qualified users shall request through \_\_\_\_\_."
- (5) "All distribution of this report is controlled. Qualified DDC users shall request through \_\_\_\_\_."

If the report has been furnished to the Office of Technical Services, Department of Commerce, for sale to the public, indicate this fact and enter the price, if known.

11. **SUPPLEMENTARY NOTES:** Use for additional explanatory notes.

12. **SPONSORING MILITARY ACTIVITY:** Enter the name of the departmental project office or laboratory sponsoring (paying for) the research and development. Include address.

13. **ABSTRACT:** Enter an abstract giving a brief and factual summary of the document indicative of the report, even though it may also appear elsewhere in the body of the technical report. If additional space is required, a continuation sheet shall be attached.

It is highly desirable that the abstract of classified reports be unclassified. Each paragraph of the abstract shall end with an indication of the military security classification of the information in the paragraph, represented as (TS), (S), (C), or (U).

There is no limitation on the length of the abstract. However, the suggested length is from 150 to 225 words.

14. **KEY WORDS:** Key words are technically meaningful terms or short phrases that characterize a report and may be used as index entries for cataloging the report. Key words must be selected so that no security classification is required. Identifiers, such as equipment model designation, trade name, military project code name, geographic location, may be used as key words but will be followed by an indication of technical content. The assignment of links, rules, and weights is optional.